



Supporting Information

© Wiley-VCH 2011

69451 Weinheim, Germany

Reversible Halide-Modulated Nickel–Nickel Bond Cleavage: Metal–Metal Bonds as Design Elements for Molecular Devices**

*Steven T. Chao, Nadia C. Lara, Sibö Lin, Michael W. Day, and Theodor Agapie**

anie_201102797_sm_miscellaneous_information.pdf

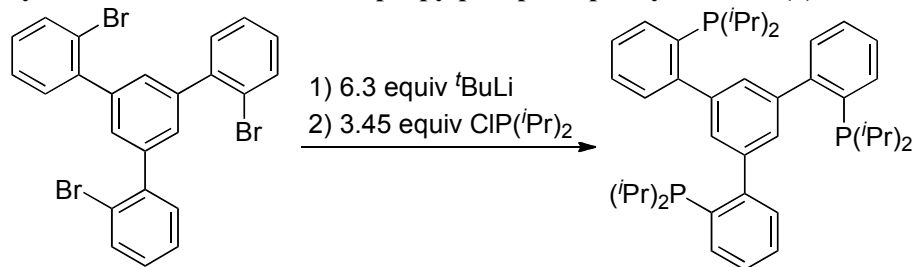
Supporting Information

I. Experimental Details	
General considerations	2
Synthesis of 1,3,5-tris-2'-diisopropylphosphinophenylbenzene (1)	2
Synthesis of [1,3,5-tris-2'-diisopropylphosphinophenylbenzene]-bis-nickel(I)chloride (2)	3
Synthesis of [1,3,5-tris-2'-diisopropylphosphinophenylbenzene]-(μ-chloro)dinickel(I) triflate (3)	4
Synthesis of 1,3-bis(2'-bromophenyl)benzene	5
Synthesis of 1,3-bis{2'-(diisopropylphosphino)phenyl}benzene (4)	5
Synthesis of [1,3-bis{2'-(diisopropylphosphino)phenyl}benzene]nickel(I)chloride (5)	6
II. Crystallographic Data	
Table 1. Crystal and refinement data for 2, 3	7
Figure 1. Structural drawing of 2.	8
Figure 2. Alternate structural drawing of 2	9
Table 2. Atomic coordinates and equivalent isotropic displacement parameters for 2	10
Table 3. Selected bond lengths for 2	11
Table 4. Anisotropic displacement parameters for 2	12
Figure 3. Structural drawing of 3.	14
Table 5. Atomic coordinates and equivalent isotropic displacement parameters for 3	15
Table 6. Selected bond lengths for 3	17
Table 7. Anisotropic displacement parameters for 3	18
Figure 4. Structural drawing of 5.	20
Table 8. Atomic coordinates and equivalent isotropic displacement parameters for 5	22
Table 9. Selected bond lengths for 5	22
Table 10. Anisotropic displacement parameters for 5	23
III. Nuclear Magnetic Resonance Spectra	
Figure 5. ¹ H NMR spectrum of 1.	24
Figure 6. ³¹ P{ ¹ H} NMR spectrum of 1.	24
Figure 7. ¹³ C{ ¹ H} NMR spectrum of 1.	25
Figure 8. gHSQC of 1	25
Figure 9. gHMBC of 1	26
Figure 10. ¹ H NMR spectrum of 2.	26
Figure 11. ¹³ C{ ¹ H} NMR spectrum of 2.	27
Figure 12. Variable temperature ¹ H NMR spectra of 2.	28
Figure 13. ¹ H NMR spectrum of 2-d ₃ .	28
Figure 14. ³¹ P{ ¹ H} NMR spectrum of 2 at -70°C and -85°C.	29
Figure 15. gCOSY spectrum of 2.	29
Figure 16. ¹ H NMR spectrum of 3.	30
Figure 17. ³¹ P{ ¹ H} NMR spectrum of 3.	30
Figure 18. ¹³ C{ ¹ H} NMR spectrum of 3.	31
Figure 19. Variable temperature ¹ H NMR spectra of 3.	31
Figure 20. Variable temperature ³¹ P{ ¹ H} NMR spectra of 3.	32
Figure 21. ¹ H NMR spectrum of 3-d ₃ .	33
Figure 22. ¹ H NMR spectrum of 1,3-bis(2'-bromophenyl)benzene	34
Figure 23. ¹³ C{ ¹ H} NMR spectrum of 1,3-bis(2'-bromophenyl)benzene	34
Figure 24. ¹ H NMR spectra of 4.	35
Figure 25. ³¹ P{ ¹ H} NMR spectra of 4.	35
Figure 26. ¹³ C{ ¹ H} NMR spectrum of 4.	36
Figure 27. ¹ H NMR spectra of 5.	36
IV. Electron Paramagnetic Resonance	
Method	37
Figure 28. EPR spectrum and simulation of 5.	37
V. Computational Details	
Method	38
Table 11. Optimized coordinates for 2-Me.	38
Table 12. Optimized coordinates for 5-Me.	39
VI. Molecular Crank Illustration	
Figure 29. Crank mechanism of 3.	42
References	42

I. Experimental Details

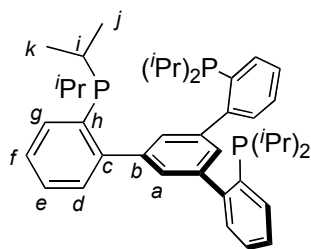
General considerations: Unless otherwise specified, all compounds were manipulated using a glove box under a nitrogen atmosphere. Solvents for all reactions were dried by Grubbs' method.¹ Benzene-*d*₆ was purchased from Cambridge Isotope Laboratories and vacuum distilled from sodium benzophenone ketyl. Dichloromethane-*d*₂ was also purchased from Cambridge Isotope Laboratories and vacuum distilled from calcium hydride. Alumina and Celite were activated by heating under vacuum at 200 °C for 12 h. 1,3,5-tris-2'-bromophenylbenzene and its isotopolog with a deuterated central arene were synthesized following literature procedures.^{2,3} All other materials were used as received. ¹H, ¹³C, ³¹P, and ¹⁹F NMR spectra were recorded on Varian Mercury 300, Varian INOVA-500, Varian INOVA-600, or Varian 400-MR spectrometers at ambient temperature, unless denoted otherwise. Chemical shifts are reported with respect to internal solvent: 7.16 ppm and 128.06 (t) ppm (C₆D₆); 7.26 ppm and 77.16 ppm (CDCl₃); and 5.32 ppm and 53.84 ppm (CD₂Cl₂) for ¹H and ¹³C NMR data, respectively. ³¹P NMR chemical shifts are reported with respect to an external 85% H₃PO₄ reference standard (0 ppm) except for variable temperature NMR data, for which standardization is software-determined based upon solvent. ¹⁹F NMR chemical shifts are reported with respect to an external α, α, α-trifluorotoluene reference standard (-63.72 ppm). Elemental analysis was performed by Midwest Microlab, LLC (Indianapolis, IN). UV-Vis spectra were collected on a Varian Cary 50 spectrophotometer using a quartz cell.

Synthesis of 1,3,5-tris-2'-diisopropylphosphinophenylbenzene (1)

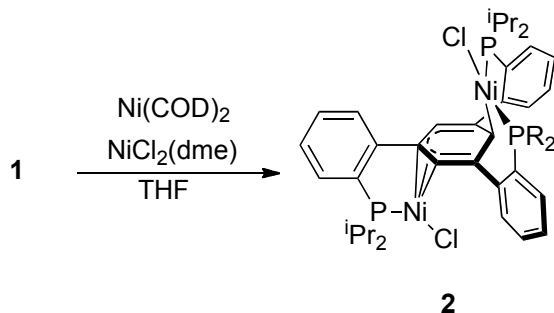


A 100 mL round bottom flask was charged with a magnetic stirbar and a 1,3,5-tris-2'-bromophenylbenzene (2.2996 g, 4.234 mmol, 1.0 equiv) solution in THF (40 mL). The flask was then placed in the coldwell and the solution frozen at liquid nitrogen temperature. Upon freezing, the flask was removed from the coldwell and ^tBuLi (1.7 M in pentane, 15.7 mL, 26.676 mmol, 6.3 equiv) was added dropwise to the thawing solution. The resulting dark red solution was then allowed to stir for 30 minutes before being being frozen again. Separately, a 250 mL round bottom flask was charged with a magnetic stirbar and a diisopropylchlorophosphine (2.33 mL, 14.608 mmol, 3.45 equiv) solution in THF (60 mL). The just-thawed lithiation reaction mixture was added dropwise to the thawing chlorophosphine solution. The reaction mixture was allowed to warm to and stir at ambient temperature for 6 hours. Volatile

materials were removed under vacuum and the remaining oil redissolved in hexanes and filtered through a bed of alumina. Volatile materials were removed from the filtrate under vacuum and the residue was redissolved in hexanes and filtered through a activated alumina again. Removal of volatile materials *in vacuo* yielded triphosphine **1** as a pale yellow oil (2.2362 g, 3.415 mmol) in 80.7% yield in around 95% purity, as determined by ^{31}P NMR spectroscopy, and used without further purification. ^1H NMR (600 MHz, CDCl_3) δ : 7.67 (app dt, 3H, aryl-*H*), 7.62 (ddd, 3H, aryl-*H*, $J = 7.6, 3.8, 1.3$ Hz), 7.47 (td, 3H, aryl-*H*, $J = 7.4, 1.2$ Hz), 7.45 (app d, 3H, central aryl-*H*, $J = 0.6$ Hz), 7.41 (td, 3H, aryl-*H*, $J = 7.5, 1.5$ Hz), 2.17 (m, 6H, $\text{CH}(\text{CH}_3)_2$), 1.14 (dd, 18H, $\text{CH}(\text{CH}_3)_2$, $J = 14.2, 7.0$ Hz), 1.03 (dd, 18H, $\text{CH}(\text{CH}_3)_2$, $J = 11.7, 6.8$ Hz). ^{31}P (121 MHz, C_6D_6) δ : -4.4. ^{13}C NMR (151 MHz, CDCl_3) (assignments with figure below) δ : 150.65 (d, $J_{\text{P-C}} = 27.5$ Hz, *h*), 140.5 (d, $J_{\text{P-C}} = 5.9$ Hz, *b*), 135.32 (d, $J_{\text{P-C}} = 24.0$ Hz, *c*), 132.40 (d, $J_{\text{P-C}} = 2.2$ Hz, *d*), 131.97 (t, $J_{\text{P-C}} = 4.5$ Hz, *a*), 130.86 (d, $J_{\text{P-C}} = 5.4$ Hz, *g*), 128.25 (s, *f*), 126.37 (s, *e*), 24.93 (d, $J_{\text{P-C}} = 15.9$ Hz, *i*), 20.50 (d, $J_{\text{P-C}} = 19.7$ Hz, *j*), 20.13 (d, $J_{\text{P-C}} = 12.4$ Hz, *k*).



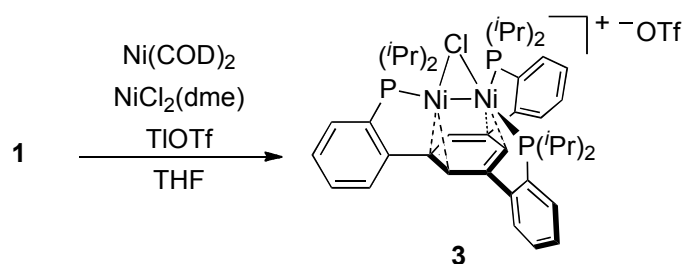
Synthesis of [1,3,5-tris-2'-diisopropylphosphinophenylbenzene]-bis-nickel(I)chloride (**2**) from **1**.



A 20 mL scintillation vial was charged with a solution of **1** (0.40858 g, 0.131 mmol, 1.0 equiv) in THF (5 mL) and a magnetic stirbar. $\text{Ni}(\text{COD})_2$ (0.0360, 0.131 mmol, 1.0 equiv) (COD = 1,5-cyclooctadiene) was added as a suspension in THF (3 mL) and allowed to stir for 20 min and reach a red-brown color, at which point a suspension of $\text{NiCl}_2(\text{dme})$ (0.0288 g, 0.131 mmol, 1.0 equiv) (dme = dimethoxyethane) in THF (3 mL) was added to the reaction mixture. After stirring for 4 hours, the dark brown solution was filtered through Celite then concentrated under vacuum. The residue was recrystallized from THF/hexanes at -35°C to produce X-ray quality crystals of **2** (0.0285 g, 0.0338 mmol, 25.8%). ^1H NMR (300 MHz, C_6D_6) δ : 9.44 (d, 2H, aryl-*H*, $J = 7.5$ Hz), 8.48 (d, 1H, aryl-*H*, $J = 7.5$ Hz), 7.34 (t, 2H, aryl-*H*,

$J = 7.4$ Hz), 7.22 (t, 2H, aryl- H , $J = 7.4$ Hz), 7.10 (t, 1H, aryl- H , $J = 7.4$ Hz), 7.02 (m, 3H, aryl- H), 6.80 (d, 1H, aryl- H , $J = 7.5$ Hz), 5.09 (br s, 2H, $\text{CH}(\text{CH}_3)_2$), 4.99 (s, 2H, central aryl- H), 4.39 (br s, 2H, $\text{CH}(\text{CH}_3)_2$), 3.29 (m, 2H, $\text{CH}(\text{CH}_3)_2$), 1.58 (d, 6H, $\text{CH}(\text{CH}_3)_2$, $J = 6.7$ Hz), 1.50 (d, 6H, $\text{CH}(\text{CH}_3)_2$, $J = 6.9$ Hz), 1.46 (d, 6H, $\text{CH}(\text{CH}_3)_2$, $J = 6.9$ Hz), 1.36 (d, 6H, $\text{CH}(\text{CH}_3)_2$, $J = 6.8$ Hz), 1.14 (d, 6H, $\text{CH}(\text{CH}_3)_2$, $J = 6.8$ Hz), 0.75 (d, 6H, $\text{CH}(\text{CH}_3)_2$, $J = 6.8$ Hz), -1.11 (br s, 1H, central aryl- H). ^{31}P (121 MHz, C_6D_6 , 25°C) no signal observed. ^{31}P (121 MHz, CD_2Cl_2 , -85°C) δ : 41.3 (br s, 1P), 0.0 (br s, 2P). ^{13}C NMR (126 MHz, C_6D_6) δ : 153.78 (s), 135.00 (s), 134.37 (s), 130.72 (s), 130.59 (s), 129.71 (s), 129.17 (s), 128.59 (s), 127.63 (s), 126.61 (s), 125.72 (s), 110.38 (s), 31.29 (s), 30.26 (s), 23.17 (s), 21.92 (s), 21.01 (s), 20.95 (s), 20.44 (s), 19.08 (s), 16.75 (s). $\mu_{\text{eff}} = 0.40$ B.M (Evans' method, 25 °C, C_6D_6). UV-Vis (THF, λ_{max}): 323; 446 nm. Anal. Calcd. for $\text{C}_{42}\text{H}_{57}\text{Cl}_2\text{P}_3\text{Ni}_2$ (%): C, 59.83; H, 6.81. Found: C, 59.72; H, 6.60.

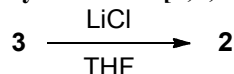
Synthesis of [1,3,5-tris-2'-diisopropylphosphinophenylbenzene]-(μ -chloro)dinickel(I) triflate (**3**) from **1**.



A 250 mL round bottom flask was charged with **1** (2.2362 g, 3.415 mmol, 1 equiv) in THF (75 mL) and a magnetic stirbar. A suspension of $\text{Ni}(\text{COD})_2$ (0.9393g, 3.415 mmol, 1 equiv) in THF (15 mL) was then added and stirred for 15 minutes, after which suspension of $\text{NiCl}_2(\text{dme})$ (0.7503 g, 3.415 mmol, 1 equiv) in THF (25 mL) was added. After the reaction mixture was stirred for 4 hours, a THF (10 mL) solution of TiOTf (1.2070 g, 3.415 mmol, 1 equiv) was added and the mixture was stirred for 3 hours. The reaction mixture was then filtered through Celite and the solvent removed under vacuum. The residue was suspended in benzene then filtered and the solids collected on a sintered glass frit and dried under vacuum to give a brown powder (2.0378 g, 2.130 mmol, 62%). Recrystallization from a mixture of dichloromethane/hexanes at -35°C gave X-ray quality crystals of **3**. ^1H NMR (500 MHz, CD_2Cl_2 , 25°C) δ : 7.57 (br), 5.87 (br), 2.56 (br), 1.15 (br). ^1H NMR (500 MHz, CD_2Cl_2 , -55°C, see Figure 17) δ : 7.63 (br, 2H, aryl- H), 7.60 (br, 2H, aryl- H), 7.47 (m, 8H, aryl- H), 5.90 (br, 2H, central aryl- H), 3.68 (br, 1H, central aryl- H), 2.85 (s, 2H, $\text{CH}(\text{CH}_3)_2$), 2.40 (br, 2H, $\text{CH}(\text{CH}_3)_2$), 1.92 (s, 2H, $\text{CH}(\text{CH}_3)_2$), 1.39 (s, 6H, $\text{CH}(\text{CH}_3)_2$), 1.15 (m, 6H, $\text{CH}(\text{CH}_3)_2$), 1.08 (br, 6H, $\text{CH}(\text{CH}_3)_2$), 0.95 (m, 6H, $\text{CH}(\text{CH}_3)_2$), 0.88 (m, 6H, $\text{CH}(\text{CH}_3)_2$), 0.80 (br, 6H, $\text{CH}(\text{CH}_3)_2$). ^{31}P (202 MHz, CD_2Cl_2 , 25°C) δ : 32.5 (br), 28.7 (br). ^{31}P (202 MHz, CD_2Cl_2 , -85°C, see Figure 18) δ : 19.5 (app t), 14.3 (dd), 7.4 (dd). ^{19}F (376 MHz, CD_2Cl_2 , 25°C) δ : -78.75 (s). ^{13}C NMR (101 MHz, CD_2Cl_2 , 40°C) δ 147.69 (br), 132.28 (br), 131.86 (br), 130.01 (s), 129.19 (s),

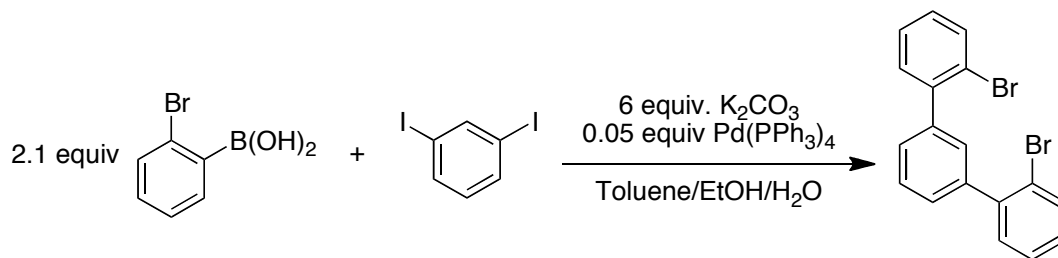
25.85 (br), 19.81 (s), 18.49 (s). $\mu_{\text{eff}} = 0.46$ B.M (Evans' method, 25 °C, CD_2Cl_2). UV-Vis (CH_2Cl_2 , λ_{max}): 248; 335; 405 nm. Anal. Calcd. for $\text{C}_{42}\text{H}_{57}\text{Cl}_2\text{P}_3\text{Ni}_2$ (%): C, 54.10; H, 5.81. Found: C, 52.59; H, 5.73.

Synthesis of [1,3,5-tris-2'-diisopropylphosphinophenylbenzene]-bis-nickel(I)chloride (2**) from **3**.**



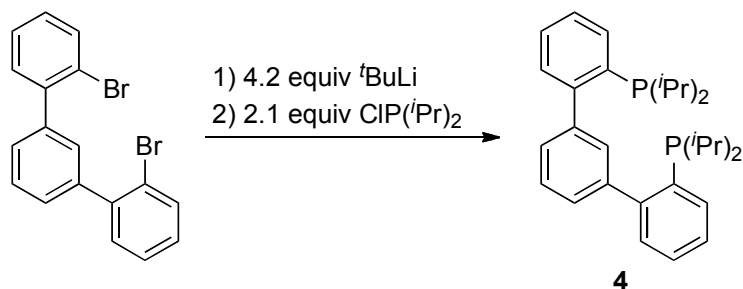
To a stirring suspension of **3** (0.6055 g, 0.633 mmol, 1 equiv) in THF (12 mL), in a 20 mL scintillation vial, was added LiCl (0.0268 g, 0.633 mmol, 1.0 equiv) suspended in THF (4 mL). After 1 hour of stirring, solvent was removed under vacuum and the residue was extracted with benzene and filtered over Celite. Removal of volatile materials from the filtrate yielded **2** (^1H and ^{31}P NMR spectroscopy).

Synthesis of 1,3-bis(2'-bromophenyl)benzene.



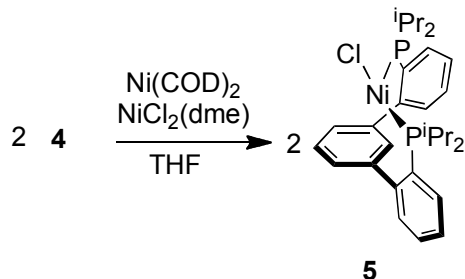
Suzuki coupling conditions were adapted from a previously published procedure.⁴ 1,3-diiodobenzene (3.00 g, 9.09 mmol, 1 equiv), 2-bromo-phenylboronic acid (3.84 g, 12.10 mmol, 2.1 equiv), K_2CO_3 (7.54 g, 54.56 mmol, 6 equiv), 165 mL toluene, 40 mL ethanol, and 40 mL water were added to a 500 mL Schlenk tube fitted with a screw-in Teflon stopper. The mixture was degassed by three freeze-pump-thaw cycles, after which $\text{Pd}(\text{PPh}_3)_4$ (525 mg, 0.46 mmol, 0.05 equiv) was added in a suspension of toluene with a counterflow of nitrogen. The reaction vessel was then placed in an oil bath pre-heated to 70°C. After stirring for 18 h the reaction mixture was allowed to cool to room temperature then extracted with three portions of CH_2Cl_2 . The combined organic fractions were dried over MgSO_4 , filtered and concentrated via rotary evaporation. Recrystallization from a concentrated CH_2Cl_2 solution and collection of the solids by filtration and drying garnered 2.12 g (50% yield, 4.55 mmol) of pale yellow crystals. ^1H NMR (300 MHz, C_6D_6) δ 7.47 (dd, 2H, aryl-*H*, $J = 8.0, 1.1$ Hz), 7.39 (app t, 1H, aryl-*H*), 7.31 (m, 2H, aryl-*H*), 7.20 (m, 1H, aryl-*H*), 7.10 (dd, 2H, aryl-*H*, $J = 7.6, 1.7$ Hz), 6.92 (td, 2H, aryl-*H*, $J = 7.5, 1.2$ Hz), 6.74 (m, 2H, aryl-*H*). ^{13}C NMR (126 MHz, CDCl_3) δ 142.37 (s), 140.87 (s), 133.28 (s), 131.51 (s), 130.64 (s), 128.95 (s), 128.69 (s), 127.74 (s), 127.53 (s), 122.77 (s). MS (m/z): calcd, 387.9 (M^+); found 388 (GC-MS, M^+).

Synthesis of 1,3-bis(2'-(diisopropylphosphino)phenyl)benzene (**4**).



A mixture of 1,3-bis(2'-bromophenyl)benzene (1.20 g, 3.08 mmol, 1 equiv) and THF (8 mL) in a 20 mL vial was frozen in a cold well. The vial was removed from the cold well and $t\text{BuLi}$ in pentane (1.7 M, 7.6 mL, 12.95 mmol, 4.2 equiv) was added via syringe to the thawing solution. The resulting green-grey mixture was stirred for 1 h and allowed to warm to room temperature. Chlorodiisopropylphosphine (0.99 g, 6.48 mmol, 2.1 equiv) was then added via syringe to the reaction mixture, which became a yellow solution within minutes. After stirring at room temperature for 2 h, the volatile materials were removed under vacuum and the residue was dissolved in toluene and filtered through Celite. The volatiles were removed from the filtrate under reduced pressure, and the resulting solids were collected on a sintered glass frit and washed with cold hexanes to yield 0.62 g (43% yield, 1.32 mmol) of spectroscopically pure **1** as a white solid. ^1H NMR (400 MHz, CD_2Cl_2) δ 7.61 (m, 2H, aryl-*H*), 7.37 (m, 6H, aryl-*H*), 7.34 (app d, 1H, aryl-*H*), 7.29 (m, 2H, aryl-*H*), 7.23 (br s, 1H, aryl-*H*), 2.06 (app sep, 4H, $\text{CH}(\text{CH}_3)_2$), 0.97 (m, 24H, $\text{CH}(\text{CH}_3)_2$). ^{31}P NMR (121 MHz, C_6D_6) δ -4.4. ^{13}C NMR (101 MHz, CD_2Cl_2) δ 150.79 (d, $J_{\text{P-C}} = 28.2$ Hz), 142.63 (d, $J_{\text{P-C}} = 6.1$ Hz), 135.42 (d, $J_{\text{P-C}} = 21.9$ Hz), 133.06 (d, $J_{\text{P-C}} = 3.0$ Hz), 130.68 (d, $J_{\text{P-C}} = 5.4$ Hz), 129.82 (d, $J_{\text{P-C}} = 5.8$ Hz), 128.70 (s), 127.00 (s), 126.24 (s), 25.40 (d, $J_{\text{P-C}} = 14.6$ Hz), 20.62 (d, $J_{\text{P-C}} = 19.9$ Hz), 20.01 (d, $J_{\text{P-C}} = 11.1$ Hz).

Synthesis of [1,3-bis{2'-(diisopropylphosphino)phenyl}benzene]nickel(I)chloride (**5**).



$\text{Ni}(\text{COD})_2$ (0.094 g, 0.34 mmol, 0.5 equiv) was added to a colorless solution of **4** (0.31 g, 0.68 mmol, 1 equiv) in THF (20 mL) leading to color changed to red-brown upon addition. The mixture was stirred at room temperature for 30 min, then $\text{NiCl}_2(\text{dme})$ (0.075 g, 0.34 mmol, 0.5 equiv) was added. The mixture

was stirred for 12 h and its color changed to bright orange over time. Volatiles were removed under reduced pressure to yield an orange powder, which was collected by filtration and washed with diethyl ether to yield 0.23 g of **5** as a bright orange powder (60% yield, 0.41 mmol). X-ray quality crystals were grown from a mixture of diethyl ether and hexanes at -35°C. ¹H NMR (400 MHz, C₆D₆) δ 52.94 (v_{1/2} = 1230 Hz), 26.87 (v_{1/2} = 981 Hz), 25.94 (v_{1/2} = 389 Hz), 17.19 (v_{1/2} = 109 Hz), 14.13 (v_{1/2} = 48 Hz), 7.53 (v_{1/2} = 20.Hz), 4.10 (v_{1/2} = 83 Hz), 3.24 (v_{1/2} = 373 Hz), 1.60 (v_{1/2} = 351 Hz), -3.56 (v_{1/2} = 96 Hz), -33.99 (v_{1/2} = 1737 Hz). ³¹P (121 MHz, C₆D₆) no signal observed. ¹³C (126 MHz, C₆D₆) no signal observed. Anal. Calcd. for C₃₀H₄₀ClP₂Ni (%): C, 64.72; H, 7.24. Found: C, 64.71; H, 7.22.

II. Crystallographic Data

Crystallographic data have been deposited at the CCDC, 12 Union Road, Cambridge CB2 1EZ, UK and copies can be obtained on request, free of charge, by quoting the publication citation and the deposition numbers 725871, 753556 and 811626.

Table 1. Crystal and refinement data for **2**, **3** and **5**.

	2	3	5
empirical formula	C ₄₂ H ₅₇ Cl ₂ P ₃ Ni ₂ •3(C ₄ H ₈ O)	[C ₄₂ H ₅₇ ClP ₃ Ni ₂] ⁺ [CF ₃ O ₃ S] ⁻ •CH ₂ Cl ₂	C ₃₀ H ₄₀ ClP ₂ Ni•C ₇ H ₈
formula wt	1059.42	1041.65	648.85
T (K)	100(2)	100(2)	100(2)
a, Å	14.1051(6)	11.5041(4)	11.1866(5)
b, Å	17.5588(8)	15.2639(6)	11.2026(5)
c, Å	22.6163(10)	15.5310(6)	15.7377(7)
α, deg	90	113.273(2)	101.346(2)
β, deg	105.019(2)	93.764(2)	93.771(3)
γ, deg	90	107.292(2)	116.475(2)
V, Å³	5410.0(4)	2339.37(15)	1704.23(13)
Z	4	2	2
cryst syst	monoclinic	triclinic	triclinic
space group	P2 ₁ /c	P-1	P-1
d_{calcd}, g/cm³	1301	1479	1264
θ range, deg	1.86-32.03	1.46-35.16	2.07-34.58
μ, mm⁻¹	0.924	1.174	0.766
abs cor	none	none	none
GOF	2.130	1.442	1.866
R1,^a wR2^b (I > 2σ(I))	0.0425, 0.0931	0.0367, 0.0554	0.0319, 0.0469

$$^a R1 = \Sigma ||F_0| - |F_c|| / \Sigma |F_0|. \quad ^b wR2 = \{ \Sigma [w(F_0^2 - F_c^2)^2] / \Sigma \}$$

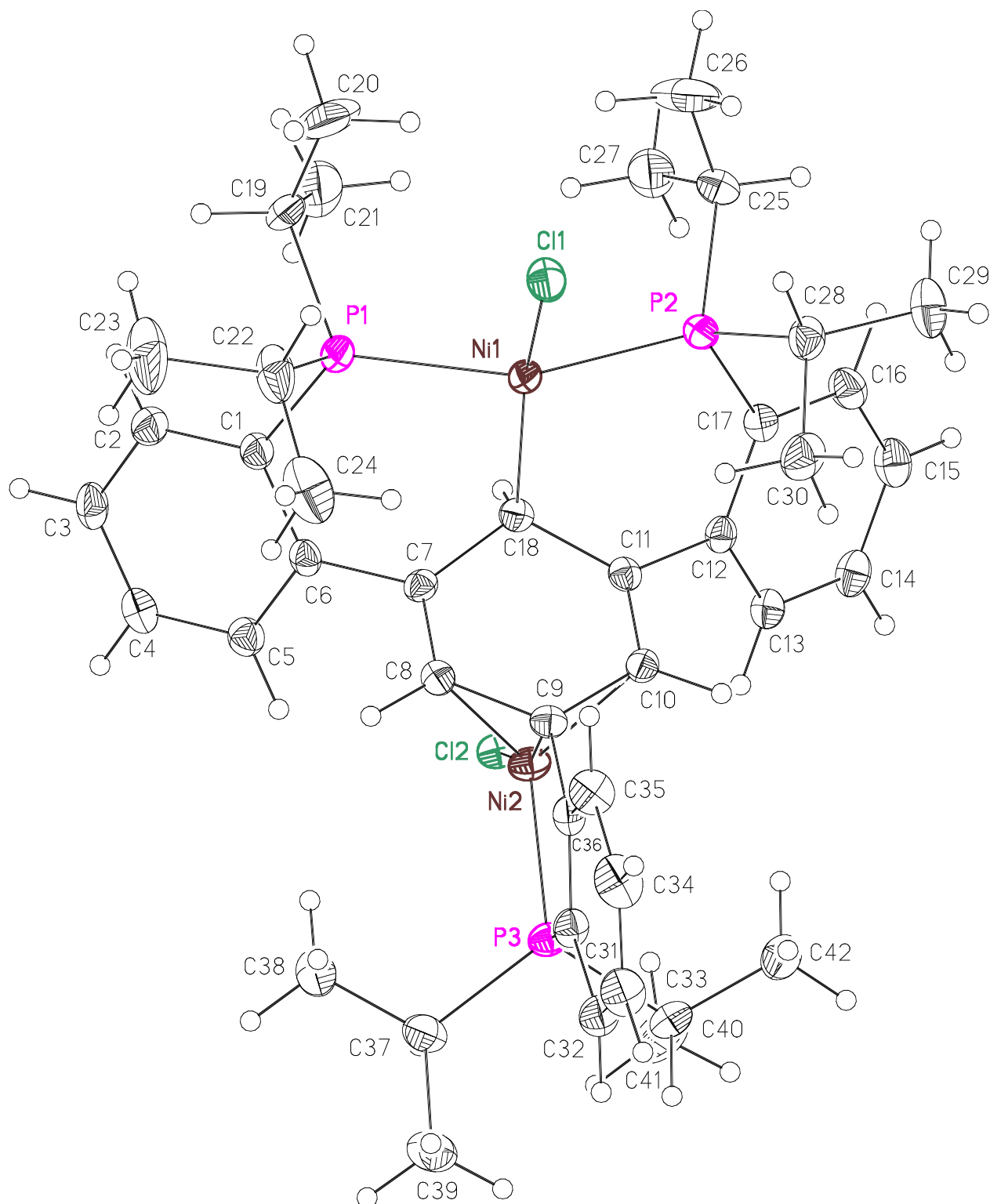


Figure 1. Structural drawing of **2** with 50% thermal probability ellipsoids.

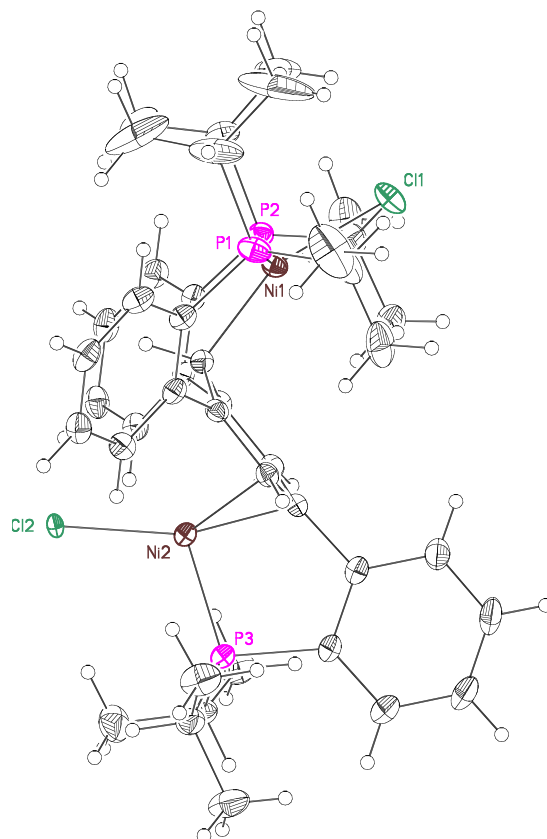


Figure 2. Alternate structural drawing of **2** with 50% thermal probability ellipsoids.

Special refinement details for 2. Crystals were mounted on a glass fiber using Paratone oil then placed on the diffractometer under a nitrogen stream at 100K. The crystal contains THF as a solvent of crystallization. This appears in the structure as three molecules per asymmetric unit, each disordered. Two types of disorder are observed, two molecules have the typical THF envelope flap and the remaining molecule is disordered over two discrete orientations. The disorder was modeled without restraints therefore some C-C distances fall outside of expected values. The choice of oxygen atom placement was based on the apparent lack hydrogen atoms in the map. The minor component account for 22-25% of the occupancy and were refined isotropically. Refinement of F^2 against ALL reflections. The weighted R-factor (wR) and goodness of fit (S) are based on F^2 , conventional R-factors (R) are based on F , with F set to zero for negative F^2 . The threshold expression of $F^2 > 2s(F^2)$ is used only for calculating R-factors(gt) etc. and is not relevant to the choice of reflections for refinement. R-factors based on F^2 are statistically about twice as large as those based on F , and R-factors based on ALL data will be even larger. All esds (except the esd in the dihedral angle between two l.s. planes) are estimated using the full covariance matrix. The cell esds are taken into account individually in the estimation of esds in distances, angles and torsion angles; correlations between esds in cell parameters are only used when they are defined by crystal symmetry. An approximate (isotropic) treatment of cell esds is used for estimating esds involving l.s. planes.

Table 2. Atomic coordinates ($\times 10^4$) and equivalent isotropic displacement parameters ($\text{\AA}^2 \times 10^3$) for **2**. $U(\text{eq})$ is defined as the trace of the orthogonalized U^{ij} tensor.

	x	y	z	U_{eq}	Occ
Ni(1)	2800(1)	7014(1)	5775(1)	17(1)	1
Ni(2)	2670(1)	9575(1)	6510(1)	19(1)	1
Cl(1)	1753(1)	6041(1)	5406(1)	25(1)	1
Cl(2)	4214(1)	9964(1)	6755(1)	15(1)	1
P(1)	3308(1)	6443(1)	6682(1)	23(1)	1
P(2)	2891(1)	7320(1)	4833(1)	18(1)	1
P(3)	1711(1)	10450(1)	6700(1)	18(1)	1
C(1)	3923(1)	7064(1)	7311(1)	19(1)	1
C(2)	4620(1)	6811(1)	7834(1)	24(1)	1
C(3)	5033(1)	7314(1)	8301(1)	24(1)	1
C(4)	4761(1)	8070(1)	8256(1)	23(1)	1
C(5)	4074(1)	8331(1)	7740(1)	21(1)	1
C(6)	3651(1)	7835(1)	7266(1)	17(1)	1
C(7)	2959(1)	8136(1)	6708(1)	16(1)	1
C(8)	2098(1)	8486(1)	6747(1)	17(1)	1
C(9)	1511(1)	8918(1)	6251(1)	17(1)	1
C(10)	1846(1)	8975(1)	5705(1)	16(1)	1
C(11)	2715(1)	8631(1)	5671(1)	16(1)	1
C(12)	3149(1)	8842(1)	5154(1)	17(1)	1
C(13)	3417(1)	9593(1)	5091(1)	20(1)	1
C(14)	3859(1)	9800(1)	4633(1)	23(1)	1
C(15)	4034(1)	9252(1)	4232(1)	25(1)	1
C(16)	3760(1)	8505(1)	4287(1)	24(1)	1
C(17)	3316(1)	8285(1)	4748(1)	18(1)	1
C(18)	3226(1)	8074(1)	6120(1)	17(1)	1
C(19)	4212(2)	5666(1)	6718(1)	47(1)	1
C(20)	3755(3)	5004(2)	6301(1)	100(2)	1
C(21)	5139(2)	5965(2)	6581(1)	70(1)	1
C(22)	2305(2)	5998(1)	6955(1)	37(1)	1
C(23)	2650(2)	5590(2)	7572(1)	56(1)	1
C(24)	1515(2)	6588(2)	6967(1)	42(1)	1
C(25)	3724(2)	6720(1)	4520(1)	27(1)	1
C(26)	3407(2)	5882(1)	4473(1)	50(1)	1
C(27)	4784(2)	6809(2)	4894(1)	38(1)	1
C(28)	1706(2)	7261(1)	4245(1)	24(1)	1
C(29)	1741(2)	7469(1)	3593(1)	36(1)	1
C(30)	938(2)	7751(1)	4445(1)	31(1)	1
C(31)	508(1)	9995(1)	6478(1)	19(1)	1
C(32)	-406(1)	10331(1)	6452(1)	25(1)	1
C(33)	-1263(1)	9928(1)	6228(1)	29(1)	1
C(34)	-1228(2)	9184(1)	6034(1)	31(1)	1
C(35)	-335(1)	8836(1)	6050(1)	26(1)	1
C(36)	534(1)	9246(1)	6268(1)	18(1)	1
C(37)	1942(2)	10765(1)	7502(1)	26(1)	1
C(38)	2123(2)	10077(1)	7927(1)	36(1)	1
C(39)	1151(2)	11283(1)	7645(1)	39(1)	1
C(40)	1557(1)	11331(1)	6244(1)	24(1)	1
C(41)	2525(2)	11772(1)	6395(1)	39(1)	1

C(42)	1226(2)	11145(1)	5560(1)	31(1)	1
C(51)	2452(3)	3227(3)	5003(2)	56(2)	0.775(11)
C(51B)	2362(13)	2960(10)	4629(11)	70(6)	0.225(11)
C(52)	2372(3)	3934(2)	4690(2)	81(1)	1
C(53)	1309(3)	4113(2)	4521(2)	69(1)	1
C(54)	839(2)	3353(2)	4449(1)	58(1)	1
O(55)	1528(2)	2838(1)	4781(1)	90(1)	1
C(61A)	3640(3)	3262(4)	7864(2)	41(1)	0.729(4)
C(62A)	3719(4)	3736(3)	8427(2)	36(1)	0.729(4)
C(63A)	3702(3)	3123(2)	8912(2)	38(1)	0.729(4)
C(64A)	3030(3)	2545(2)	8568(2)	47(1)	0.729(4)
O(65A)	3059(2)	2572(2)	7946(1)	56(1)	0.729(4)
C(61B)	3580(20)	3492(16)	7816(13)	132(13)	0.271(4)
C(62B)	3419(13)	3808(12)	8399(9)	67(7)	0.271(4)
C(63B)	3967(8)	3346(6)	8880(5)	33(3)	0.271(4)
C(64B)	4210(6)	2662(5)	8649(4)	34(2)	0.271(4)
O(65B)	3813(13)	2699(10)	8005(7)	143(6)	0.271(4)
O(71)	573(4)	3889(3)	7120(2)	193(2)	1
C(72)	900(2)	3241(2)	6774(2)	69(1)	1
C(73)	1190(3)	3652(3)	6305(2)	90(1)	1
C(74)	506(3)	4283(2)	6112(2)	75(1)	1
C(75A)	92(7)	4408(6)	6606(4)	78(3)	0.777(19)
C(75B)	326(7)	4712(8)	6814(6)	19(3)	0.223(19)

Table 3. Selected bond lengths [\AA] and angles [$^\circ$] for **2**.

Ni(1)-C(18)	2.0473(18)	C(18)-Ni(1)-P(1)	93.79(5)
Ni(1)-P(1)	2.2283(5)	C(18)-Ni(1)-P(2)	93.48(5)
Ni(1)-P(2)	2.2331(5)	P(1)-Ni(1)-P(2)	154.49(2)
Ni(1)-Cl(1)	2.2708(5)	C(18)-Ni(1)-Cl(1)	157.33(5)
Ni(2)-C(9)	1.9614(18)	P(1)-Ni(1)-Cl(1)	91.31(2)
Ni(2)-P(3)	2.1612(5)	P(2)-Ni(1)-Cl(1)	91.323(19)
Ni(2)-C(10)	2.1629(18)	C(9)-Ni(2)-P(3)	87.77(5)
Ni(2)-C(8)	2.1951(17)	C(9)-Ni(2)-C(10)	40.40(6)
Ni(2)-Cl(2)	2.2118(5)	P(3)-Ni(2)-C(10)	106.66(5)
		C(9)-Ni(2)-C(8)	39.67(7)
		P(3)-Ni(2)-C(8)	106.43(5)
		C(10)-Ni(2)-C(8)	68.25(7)
		C(9)-Ni(2)-Cl(2)	161.19(5)
		P(3)-Ni(2)-Cl(2)	110.90(2)
		C(10)-Ni(2)-Cl(2)	129.82(5)
		C(8)-Ni(2)-Cl(2)	127.44(5)

Table 4. Anisotropic displacement parameters ($\text{\AA}^2 \times 10^4$) for **2**. The anisotropic displacement factor exponent takes the form: $-2\pi^2 [h^2 a^{*2} U^{11} + \dots + 2 h k a^* b^* U^{12}]$

	U ¹¹	U ²²	U ³³	U ²³	U ¹³	U ¹²
Ni(1)	198(1)	144(1)	158(1)	3(1)	35(1)	7(1)
Ni(2)	132(1)	174(1)	251(1)	-22(1)	46(1)	8(1)
Cl(1)	360(3)	173(2)	205(2)	-12(2)	42(2)	-83(2)
Cl(2)	104(2)	143(2)	200(2)	-28(2)	18(2)	-40(2)
P(1)	333(3)	157(2)	174(2)	20(2)	40(2)	32(2)
P(2)	184(2)	181(2)	162(2)	-11(2)	46(2)	10(2)
P(3)	148(2)	175(2)	216(2)	-7(2)	42(2)	22(2)
C(1)	198(9)	225(10)	165(8)	16(8)	60(8)	29(8)
C(2)	250(10)	269(11)	218(9)	37(9)	78(8)	76(9)
C(3)	175(9)	381(12)	160(9)	52(9)	23(8)	46(9)
C(4)	216(10)	300(11)	170(9)	-6(8)	46(8)	-44(8)
C(5)	230(10)	208(10)	196(9)	4(8)	65(8)	-15(8)
C(6)	163(9)	225(10)	148(8)	18(8)	68(7)	8(7)
C(7)	177(9)	130(9)	177(8)	2(7)	32(7)	-5(7)
C(8)	178(9)	162(9)	168(8)	-3(7)	50(7)	-27(7)
C(9)	153(8)	157(9)	195(9)	-30(7)	41(7)	-21(7)
C(10)	178(9)	143(9)	160(8)	-3(7)	19(7)	-8(7)
C(11)	163(8)	159(9)	152(8)	-17(7)	27(7)	-27(7)
C(12)	141(8)	195(9)	157(8)	23(7)	25(7)	7(7)
C(13)	199(9)	217(10)	181(9)	19(8)	28(8)	0(8)
C(14)	201(9)	242(10)	225(9)	55(8)	16(8)	-40(8)
C(15)	207(9)	338(12)	212(9)	41(9)	74(8)	-40(9)
C(16)	234(10)	288(11)	204(9)	-1(9)	94(8)	-3(9)
C(17)	166(9)	211(9)	173(8)	7(8)	44(7)	-4(7)
C(18)	159(8)	176(9)	173(8)	-12(7)	39(7)	-1(7)
C(19)	780(20)	292(13)	242(11)	2(10)	-33(12)	313(13)
C(20)	1580(40)	456(19)	576(19)	-267(16)	-410(20)	650(20)
C(21)	730(20)	990(30)	421(15)	197(17)	261(16)	670(20)
C(22)	578(16)	290(12)	223(10)	41(10)	73(11)	-185(11)
C(23)	820(20)	514(17)	306(12)	155(13)	81(14)	-257(16)
C(24)	369(13)	575(17)	337(12)	-4(12)	150(11)	-229(12)
C(25)	313(11)	279(11)	248(10)	-28(9)	129(9)	66(9)
C(26)	659(18)	268(13)	698(18)	-121(13)	423(16)	51(12)
C(27)	326(12)	530(15)	320(11)	38(11)	128(10)	172(11)
C(28)	243(10)	248(10)	197(9)	9(8)	1(8)	-17(8)
C(29)	373(13)	480(15)	193(10)	44(10)	-15(10)	-41(11)
C(30)	225(10)	329(12)	312(11)	15(10)	-18(9)	33(9)
C(31)	144(8)	237(10)	191(9)	16(8)	32(7)	11(8)
C(32)	196(9)	304(11)	241(10)	22(9)	61(8)	60(8)
C(33)	154(9)	445(14)	285(11)	7(10)	59(9)	48(9)
C(34)	153(9)	455(14)	316(11)	-31(11)	36(9)	-68(9)
C(35)	198(10)	305(11)	288(10)	-25(9)	60(9)	-38(9)
C(36)	152(8)	245(10)	156(8)	21(8)	40(7)	4(8)
C(37)	234(10)	290(11)	248(10)	-68(9)	50(9)	28(9)
C(38)	428(14)	421(14)	232(10)	23(10)	79(10)	122(11)
C(39)	399(13)	448(14)	315(11)	-77(11)	76(11)	171(11)
C(40)	216(10)	193(10)	297(10)	28(9)	59(9)	47(8)

C(41)	326(13)	246(12)	553(15)	80(11)	35(12)	-37(10)
C(42)	359(12)	282(11)	292(11)	72(9)	101(10)	60(10)
C(51)	370(20)	780(30)	490(30)	230(20)	56(17)	-14(19)
C(52)	890(30)	660(20)	830(20)	-80(20)	140(20)	-390(20)
C(53)	1130(30)	343(16)	640(20)	57(15)	320(20)	176(18)
C(54)	383(15)	720(20)	615(18)	37(17)	101(14)	-27(15)
O(55)	711(16)	409(13)	1440(20)	338(15)	35(17)	-104(12)
C(61A)	321(19)	650(30)	303(19)	-20(20)	138(15)	70(20)
C(62A)	370(30)	340(20)	430(20)	7(16)	210(20)	-42(19)
C(63A)	390(20)	360(20)	395(19)	111(17)	128(17)	-12(18)
C(64A)	610(20)	316(19)	560(20)	-56(17)	290(20)	-45(17)
O(65A)	620(20)	533(18)	509(15)	-126(14)	129(14)	-140(14)
O(71)	2590(60)	1980(50)	1050(30)	-70(30)	180(30)	-1070(40)
C(72)	504(18)	850(30)	700(20)	420(20)	126(17)	201(18)
C(73)	520(20)	1330(40)	870(20)	470(30)	190(20)	140(20)
C(74)	610(20)	840(30)	670(20)	260(20)	-71(17)	-317(19)
C(75A)	1150(50)	690(50)	620(40)	120(40)	460(40)	400(40)

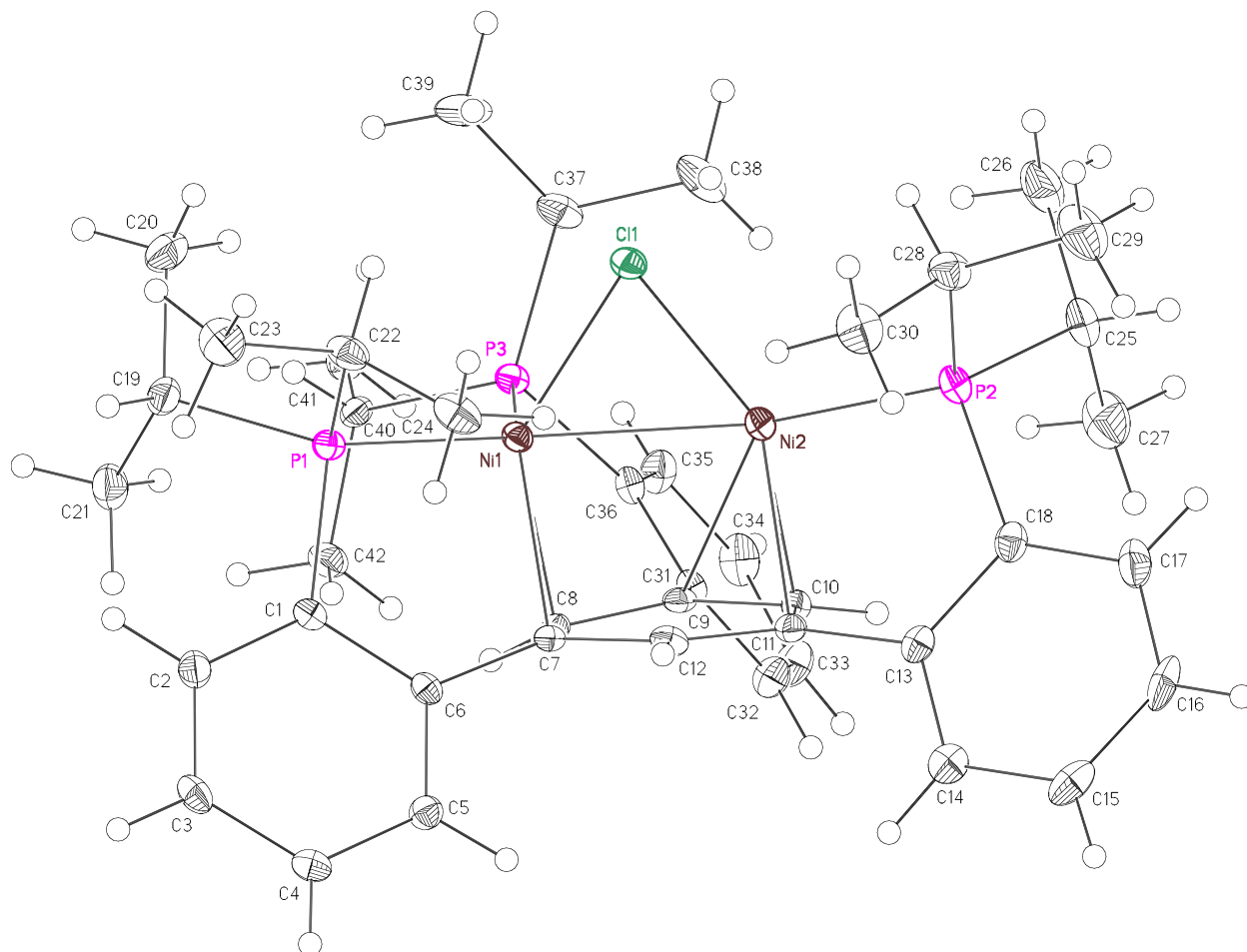


Figure 3. Structural drawing of **3** with 50% thermal probability ellipsoids. Triflate counteranion is not shown for clarity.

Special refinement details for 3. Crystals were mounted on a glass fiber using Paratone oil then placed on the diffractometer under a nitrogen stream at 100K. Refinement of F^2 against ALL reflections. The weighted R-factor (wR) and goodness of fit (S) are based on F^2 , conventional R-factors (R) are based on F , with F set to zero for negative F^2 . The threshold expression of $F^2 > 2s(F^2)$ is used only for calculating R-factors(gt) etc. and is not relevant to the choice of reflections for refinement. R-factors based on F^2 are statistically about twice as large as those based on F , and R-factors based on ALL data will be even larger. All esds (except the esd in the dihedral angle between two l.s. planes) are estimated using the full covariance matrix. The cell esds are taken into account individually in the estimation of esds in distances, angles and torsion angles; correlations between esds in cell parameters are only used when they are defined by crystal symmetry. An approximate (isotropic) treatment of cell esds is used for estimating esds involving l.s. planes.

Table 5 Atomic coordinates ($\times 10^4$) and equivalent isotropic displacement parameters ($\text{\AA}^2 \times 10^3$) for **3**. U(eq) is defined as the trace of the orthogonalized U^{ij} tensor.

	x	y	z	U _{eq}
Ni(1)	4083(1)	1931(1)	4462(1)	10(1)
Ni(2)	2876(1)	400(1)	2911(1)	13(1)
Cl(1)	3840(1)	259(1)	4056(1)	13(1)
P(1)	3932(1)	2542(1)	5999(1)	11(1)
P(2)	1786(1)	-1083(1)	1772(1)	14(1)
P(3)	5993(1)	2536(1)	4065(1)	11(1)
C(1)	2788(1)	3160(1)	6094(1)	11(1)
C(2)	2587(1)	3816(1)	6950(1)	14(1)
C(3)	1597(1)	4148(1)	6950(1)	15(1)
C(4)	775(1)	3812(1)	6096(1)	14(1)
C(5)	975(1)	3173(1)	5246(1)	13(1)
C(6)	1985(1)	2853(1)	5228(1)	10(1)
C(7)	2221(1)	2221(1)	4291(1)	10(1)
C(8)	3259(1)	2660(1)	3954(1)	10(1)
C(9)	3368(1)	2113(1)	2993(1)	11(1)
C(10)	2367(1)	1242(1)	2348(1)	11(1)
C(11)	1271(1)	849(1)	2670(1)	11(1)
C(12)	1229(1)	1327(1)	3626(1)	12(1)
C(13)	203(1)	-18(1)	1935(1)	12(1)
C(14)	-918(1)	108(1)	1749(1)	16(1)
C(15)	-1882(2)	-674(1)	1007(1)	20(1)
C(16)	-1718(2)	-1571(1)	455(1)	22(1)
C(17)	-618(2)	-1716(1)	636(1)	20(1)
C(18)	353(1)	-945(1)	1386(1)	14(1)
C(19)	5206(1)	3426(1)	7052(1)	16(1)
C(20)	6209(2)	2961(2)	7068(1)	22(1)
C(21)	5739(2)	4491(1)	7106(1)	20(1)
C(22)	3163(2)	1462(1)	6296(1)	16(1)
C(23)	3097(2)	1781(1)	7349(1)	23(1)
C(24)	1863(2)	835(1)	5667(1)	19(1)
C(25)	2421(2)	-1604(1)	707(1)	19(1)
C(26)	3597(2)	-1776(2)	997(1)	26(1)
C(27)	2678(2)	-896(2)	212(1)	29(1)
C(28)	1325(2)	-2062(1)	2225(1)	18(1)
C(29)	604(2)	-3142(1)	1469(1)	29(1)
C(30)	624(2)	-1732(1)	3021(1)	22(1)
C(31)	4433(1)	2534(1)	2606(1)	11(1)
C(32)	4184(2)	2740(1)	1829(1)	16(1)
C(33)	5132(2)	3063(1)	1399(1)	19(1)
C(34)	6325(2)	3158(1)	1718(1)	19(1)
C(35)	6586(2)	2974(1)	2498(1)	16(1)
C(36)	5660(1)	2685(1)	2972(1)	12(1)
C(37)	7017(1)	1772(1)	3772(1)	17(1)

C(38)	6385(2)	751(1)	2904(1)	24(1)
C(39)	7450(2)	1642(1)	4652(1)	24(1)
C(40)	7075(1)	3841(1)	4908(1)	12(1)
C(41)	8377(2)	4194(1)	4726(1)	17(1)
C(42)	6464(2)	4621(1)	4971(1)	18(1)
S(1)	9482(1)	5903(1)	8111(1)	17(1)
F(1)	9791(1)	7771(1)	8379(1)	41(1)
F(2)	10176(1)	6868(1)	7047(1)	40(1)
F(3)	8296(1)	6632(1)	7220(1)	37(1)
O(1)	10775(1)	6232(1)	8529(1)	31(1)
O(2)	8682(1)	6043(1)	8786(1)	26(1)
O(3)	9003(1)	4955(1)	7262(1)	26(1)
C(51)	9436(2)	6840(1)	7671(1)	22(1)
Cl(2)	2361(1)	5438(1)	-375(1)	38(1)
Cl(3)	3478(1)	3935(1)	-462(1)	38(1)
C(61)	3177(2)	5031(2)	295(1)	31(1)

Table 6. Selected bond lengths [Å] and angles [°] for **3**.

Ni(1)-C(8)	1.9961(14)	C(8)-Ni(1)-P(1)	102.70(4)
Ni(1)-P(1)	2.2331(4)	C(8)-Ni(1)-Cl(1)	135.62(4)
Ni(1)-Cl(1)	2.2954(4)	P(1)-Ni(1)-Cl(1)	103.749(15)
Ni(1)-C(7)	2.3323(14)	C(8)-Ni(1)-C(7)	37.44(5)
Ni(1)-P(3)	2.3415(4)	P(1)-Ni(1)-C(7)	81.39(3)
Ni(1)-Ni(2)	2.5248(3)	Cl(1)-Ni(1)-C(7)	114.31(4)
Ni(2)-C(10)	2.0060(14)	C(8)-Ni(1)-P(3)	94.90(4)
Ni(2)-Cl(1)	2.1503(4)	P(1)-Ni(1)-P(3)	119.159(16)
Ni(2)-P(2)	2.1642(4)	Cl(1)-Ni(1)-P(3)	102.377(15)
Ni(2)-C(11)	2.2096(14)	C(7)-Ni(1)-P(3)	132.31(4)
Ni(2)-C(9)	2.4536(14)	C(8)-Ni(1)-Ni(2)	83.96(4)
		P(1)-Ni(1)-Ni(2)	137.291(14)
		Cl(1)-Ni(1)-Ni(2)	52.727(10)
		C(7)-Ni(1)-Ni(2)	79.34(3)
		P(3)-Ni(1)-Ni(2)	101.857(12)
		C(10)-Ni(2)-Cl(1)	151.38(4)
		C(10)-Ni(2)-P(2)	97.50(4)
		Cl(1)-Ni(2)-P(2)	110.979(16)
		C(10)-Ni(2)-C(11)	39.53(5)
		Cl(1)-Ni(2)-C(11)	136.99(4)
		P(2)-Ni(2)-C(11)	85.95(4)
		C(10)-Ni(2)-C(9)	35.04(5)
		Cl(1)-Ni(2)-C(9)	117.50(3)
		P(2)-Ni(2)-C(9)	130.98(3)
		C(11)-Ni(2)-C(9)	63.74(5)
		C(10)-Ni(2)-Ni(1)	93.23(4)
		Cl(1)-Ni(2)-Ni(1)	58.152(11)
		P(2)-Ni(2)-Ni(1)	167.726(14)
		C(11)-Ni(2)-Ni(1)	98.72(4)
		C(9)-Ni(2)-Ni(1)	60.81(3)

Table 7. Anisotropic displacement parameters ($\text{\AA}^2 \times 10^4$) for **3**. The anisotropic displacement factor exponent takes the form: $-2p^2 [h^2 a^{*2} U^{11} + \dots + 2 h k a^* b^* U^{12}]$

	U ¹¹	U ²²	U ³³	U ²³	U ¹³	U ¹²
Ni(1)	111(1)	86(1)	105(1)	40(1)	24(1)	38(1)
Ni(2)	150(1)	91(1)	116(1)	29(1)	4(1)	41(1)
Cl(1)	150(2)	101(2)	151(2)	60(1)	23(1)	49(1)
P(1)	123(2)	113(2)	109(2)	50(2)	26(1)	56(2)
P(2)	149(2)	103(2)	129(2)	27(2)	28(2)	37(2)
P(3)	96(2)	96(2)	129(2)	48(2)	25(1)	37(1)
C(1)	110(7)	95(7)	125(7)	45(6)	36(5)	41(5)
C(2)	168(8)	128(7)	116(7)	42(6)	22(6)	47(6)
C(3)	192(8)	126(7)	129(7)	42(6)	75(6)	73(6)
C(4)	142(8)	145(7)	173(8)	72(6)	55(6)	79(6)
C(5)	124(7)	143(7)	119(7)	58(6)	29(6)	53(6)
C(6)	112(7)	76(6)	115(7)	43(5)	35(5)	25(5)
C(7)	111(7)	104(7)	109(7)	49(6)	21(5)	58(5)
C(8)	100(7)	80(7)	103(7)	33(6)	-8(5)	27(5)
C(9)	117(7)	101(7)	127(7)	64(6)	21(5)	56(5)
C(10)	132(7)	112(7)	93(7)	41(6)	19(5)	53(6)
C(11)	112(7)	97(7)	115(7)	48(6)	9(5)	40(5)
C(12)	110(7)	110(7)	165(7)	75(6)	50(6)	47(6)
C(13)	119(7)	135(7)	110(7)	72(6)	20(5)	18(6)
C(14)	152(8)	163(8)	170(8)	92(7)	34(6)	36(6)
C(15)	128(8)	265(9)	213(8)	155(7)	-11(6)	17(7)
C(16)	199(9)	211(9)	130(8)	71(7)	-69(6)	-49(7)
C(17)	247(9)	137(8)	134(8)	31(6)	6(6)	18(7)
C(18)	153(8)	137(7)	111(7)	56(6)	19(6)	23(6)
C(19)	156(8)	188(8)	113(7)	53(6)	16(6)	70(6)
C(20)	183(9)	277(10)	200(9)	94(8)	-5(7)	110(7)
C(21)	182(9)	177(8)	160(8)	30(7)	9(7)	42(7)
C(22)	221(9)	139(7)	180(8)	96(6)	86(6)	96(6)
C(23)	337(11)	222(9)	188(9)	130(8)	104(8)	109(8)
C(24)	216(9)	148(8)	243(9)	110(7)	117(7)	76(7)
C(25)	209(9)	151(8)	143(8)	9(6)	47(6)	43(7)
C(26)	258(10)	233(10)	228(9)	27(8)	97(8)	110(8)
C(27)	374(12)	301(11)	206(9)	111(8)	138(8)	126(9)
C(28)	167(8)	137(8)	225(8)	83(7)	30(6)	42(6)
C(29)	365(12)	131(9)	323(11)	83(8)	83(9)	34(8)
C(30)	233(10)	193(9)	235(9)	106(8)	78(7)	38(7)
C(31)	122(7)	92(7)	107(7)	29(5)	35(5)	32(5)
C(32)	138(8)	182(8)	148(7)	76(6)	22(6)	39(6)
C(33)	208(9)	232(9)	136(8)	114(7)	39(6)	54(7)
C(34)	172(8)	201(8)	160(8)	78(7)	82(6)	15(6)
C(35)	100(8)	191(8)	150(8)	56(6)	24(6)	25(6)
C(36)	129(7)	96(7)	104(7)	23(5)	25(5)	24(6)
C(37)	133(8)	134(7)	256(8)	84(7)	74(6)	65(6)
C(38)	227(10)	161(8)	304(10)	51(8)	123(8)	90(7)

C(39)	202(9)	220(9)	380(11)	169(9)	58(8)	127(8)
C(40)	110(7)	115(7)	124(7)	55(6)	-7(5)	32(6)
C(41)	138(8)	154(8)	182(8)	65(7)	12(6)	21(6)
C(42)	177(9)	116(8)	224(9)	40(7)	-5(7)	58(6)
S(1)	158(2)	158(2)	166(2)	48(2)	30(2)	56(2)
F(1)	627(8)	165(6)	362(6)	106(5)	61(5)	65(5)
F(2)	413(7)	608(8)	387(6)	361(6)	223(5)	218(6)
F(3)	304(6)	450(7)	438(6)	235(6)	4(5)	211(5)
O(1)	177(7)	359(8)	380(7)	179(6)	-49(5)	78(6)
O(2)	332(7)	210(6)	215(6)	74(5)	147(5)	65(5)
O(3)	277(7)	195(6)	233(6)	-2(5)	51(5)	106(5)
C(51)	235(9)	220(9)	182(8)	75(7)	53(7)	74(7)
Cl(2)	579(3)	260(2)	272(2)	122(2)	55(2)	116(2)
Cl(3)	395(3)	291(3)	398(3)	129(2)	90(2)	92(2)
C(61)	332(11)	304(11)	219(9)	103(8)	71(8)	36(9)

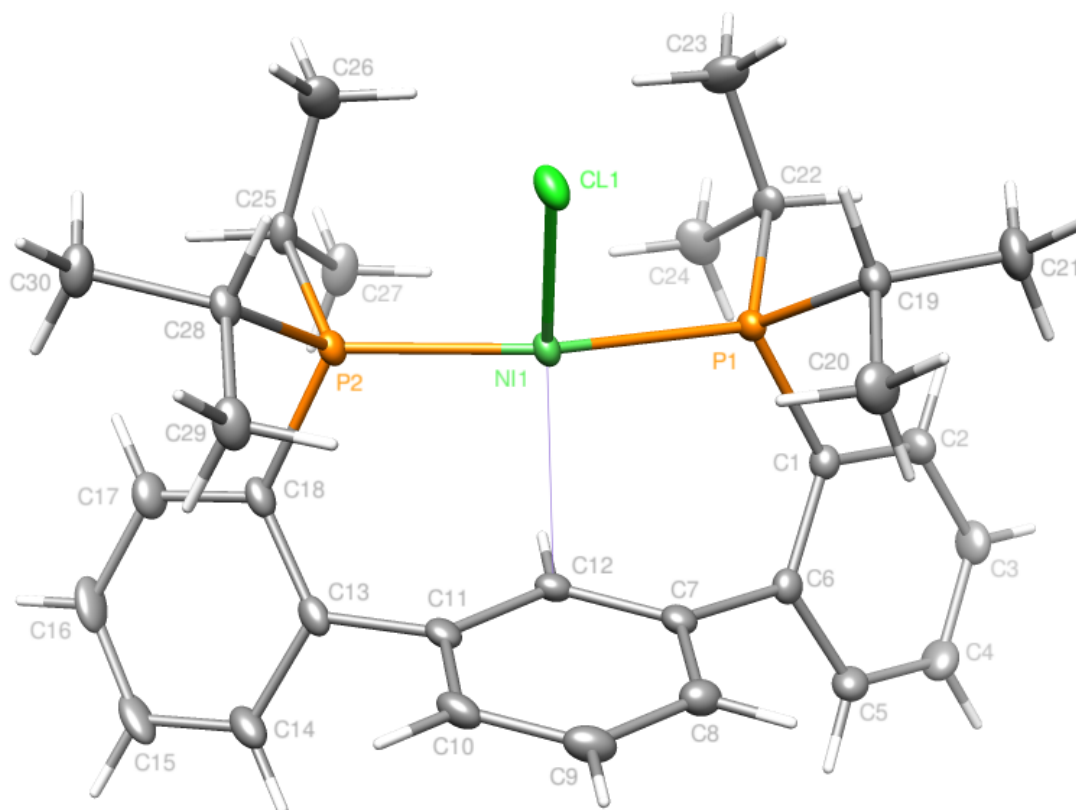


Figure 4. Structural drawing of **5** with 50% thermal probability ellipsoids.

Special Refinement Details for 5. Crystals were mounted on a glass fiber using Paratone oil then placed on the diffractometer under a nitrogen stream at 100K. Refinement of F^2 against ALL reflections. The weighted R-factor (wR) and goodness of fit (S) are based on F^2 , conventional R-factors (R) are based on F , with F set to zero for negative F^2 . The threshold expression of $F^2 > 2\sigma(F^2)$ is used only for calculating R-factors(gt) etc. and is not relevant to the choice of reflections for refinement. R-factors based on F^2 are statistically about twice as large as those based on F , and R-factors based on ALL data will be even larger. All esds (except the esd in the dihedral angle between two l.s. planes) are estimated using the full covariance matrix. The cell esds are taken into account individually in the estimation of esds in distances, angles and torsion angles; correlations between esds in cell parameters are only used when they are defined by crystal symmetry. An approximate (isotropic) treatment of cell esds is used for estimating esds involving l.s. planes.

Table 8. Atomic coordinates ($\times 10^4$) and equivalent isotropic displacement parameters ($\text{\AA}^2 \times 10^3$) for **5** (CCDC 811626). $U(\text{eq})$ is defined as the trace of the orthogonalized U^{ij} tensor.

	x	y	z	U_{eq}
Ni(1)	7745(1)	2985(1)	7683(1)	12(1)
Cl(1)	9330(1)	2234(1)	7833(1)	18(1)
P(1)	5975(1)	1089(1)	7843(1)	12(1)
P(2)	8893(1)	4584(1)	6978(1)	13(1)
C(1)	4604(1)	1297(1)	8312(1)	14(1)
C(2)	3288(1)	204(1)	8157(1)	18(1)
C(3)	2267(1)	331(1)	8551(1)	21(1)
C(4)	2553(1)	1574(1)	9124(1)	22(1)
C(5)	3847(1)	2667(1)	9294(1)	19(1)
C(6)	4884(1)	2564(1)	8886(1)	14(1)
C(7)	6239(1)	3813(1)	9083(1)	14(1)
C(8)	6962(1)	4378(1)	9936(1)	18(1)
C(9)	8179(1)	5602(1)	10146(1)	20(1)
C(10)	8650(1)	6286(1)	9499(1)	18(1)
C(11)	7946(1)	5764(1)	8643(1)	14(1)
C(12)	6751(1)	4498(1)	8431(1)	14(1)
C(13)	8362(1)	6594(1)	7979(1)	15(1)
C(14)	8414(1)	7900(1)	8186(1)	21(1)
C(15)	8736(1)	8717(1)	7596(1)	25(1)
C(16)	8990(1)	8247(1)	6787(1)	26(1)
C(17)	8974(1)	6975(1)	6578(1)	21(1)
C(18)	8685(1)	6145(1)	7176(1)	15(1)
C(19)	6463(1)	224(1)	8587(1)	15(1)
C(20)	7174(1)	1234(1)	9485(1)	23(1)
C(21)	5317(1)	-1128(1)	8683(1)	24(1)
C(22)	5088(1)	-265(1)	6806(1)	15(1)
C(23)	6087(1)	-681(1)	6378(1)	24(1)
C(24)	4428(1)	247(1)	6185(1)	25(1)
C(25)	8555(1)	3971(1)	5768(1)	17(1)
C(26)	8891(1)	2774(1)	5499(1)	24(1)
C(27)	7081(1)	3551(1)	5405(1)	25(1)
C(28)	10758(1)	5309(1)	7283(1)	14(1)
C(29)	11229(1)	6140(1)	8240(1)	20(1)
C(30)	11609(1)	6150(1)	6686(1)	21(1)
C(41)	1476(2)	1444(2)	6000(1)	72(1)
C(42)	2625(1)	2881(1)	6360(1)	38(1)
C(43)	3413(2)	3607(2)	5814(1)	45(1)
C(44)	4480(2)	4926(2)	6154(1)	42(1)
C(45)	4774(1)	5520(1)	7029(1)	39(1)
C(46)	4001(2)	4820(2)	7579(1)	45(1)
C(47)	2932(2)	3512(2)	7244(1)	44(1)

Table 9. Selected bond lengths [Å] and angles [°] for 5 (CCDC 811626).

Ni(1)-P(2)	2.2374(3)	P(2)-Ni(1)-P(1)	155.108(13)
Ni(1)-P(1)	2.2402(3)	P(2)-Ni(1)-Cl(1)	96.510(11)
Ni(1)-Cl(1)	2.2936(3)	P(1)-Ni(1)-Cl(1)	96.543(11)

Table 10. Anisotropic displacement parameters ($\text{\AA}^2 \times 10^4$) for 5 (CCDC 811626). The anisotropic displacement factor exponent takes the form: $-2p^2 [h^2 a^{*2} U^{11} + \dots + 2 h k a^* b^* U^{12}]$

	U ¹¹	U ²²	U ³³	U ²³	U ¹³	U ¹²
Ni(1)	107(1)	90(1)	158(1)	43(1)	28(1)	34(1)
Cl(1)	125(1)	120(1)	297(2)	85(1)	37(1)	52(1)
P(1)	109(1)	96(1)	143(2)	28(1)	33(1)	37(1)
P(2)	115(1)	100(1)	158(2)	48(1)	24(1)	38(1)
C(1)	114(5)	136(5)	158(6)	53(4)	36(4)	54(5)
C(2)	146(6)	136(5)	239(7)	34(5)	49(5)	42(5)
C(3)	121(6)	193(6)	297(7)	93(5)	63(5)	46(5)
C(4)	182(6)	252(6)	299(7)	117(6)	123(5)	132(6)
C(5)	216(6)	174(6)	222(6)	67(5)	90(5)	115(5)
C(6)	141(5)	142(5)	141(6)	63(4)	33(4)	70(5)
C(7)	147(5)	111(5)	171(6)	23(4)	37(5)	76(5)
C(8)	216(6)	170(6)	163(6)	34(5)	39(5)	107(5)
C(9)	220(6)	184(6)	175(6)	-21(5)	-22(5)	114(5)
C(10)	141(6)	106(5)	257(7)	-15(5)	5(5)	46(5)
C(11)	138(5)	99(5)	203(6)	18(4)	39(5)	69(5)
C(12)	146(5)	115(5)	147(6)	4(4)	18(4)	70(5)
C(13)	81(5)	104(5)	254(6)	50(5)	14(5)	25(4)
C(14)	125(6)	119(5)	365(8)	51(5)	49(5)	51(5)
C(15)	143(6)	123(5)	513(9)	117(6)	56(6)	69(5)
C(16)	184(6)	196(6)	449(9)	207(6)	70(6)	84(5)
C(17)	181(6)	187(6)	285(7)	114(5)	45(5)	79(5)
C(18)	108(5)	109(5)	232(6)	69(5)	13(5)	39(4)
C(19)	154(6)	135(5)	196(6)	75(5)	64(5)	74(5)
C(20)	290(7)	236(6)	193(6)	93(5)	29(5)	125(6)
C(21)	239(7)	192(6)	313(7)	151(5)	82(6)	80(6)
C(22)	131(5)	111(5)	167(6)	18(4)	29(5)	19(5)
C(23)	202(6)	209(6)	206(7)	-45(5)	38(5)	60(5)
C(24)	266(7)	204(6)	214(7)	17(5)	-42(6)	69(6)
C(25)	141(6)	148(5)	172(6)	64(5)	33(5)	22(5)
C(26)	305(7)	203(6)	183(6)	30(5)	61(6)	93(6)
C(27)	167(6)	284(7)	212(7)	86(5)	5(5)	26(6)
C(28)	119(5)	120(5)	197(6)	68(4)	28(5)	45(5)
C(29)	150(6)	180(6)	223(6)	76(5)	3(5)	38(5)
C(30)	133(6)	210(6)	236(7)	92(5)	31(5)	26(5)
C(41)	360(10)	408(10)	1300(20)	333(11)	44(11)	60(9)
C(42)	243(8)	379(8)	555(11)	223(8)	78(7)	140(7)
C(43)	459(10)	424(9)	333(9)	63(7)	81(8)	115(8)
C(44)	356(9)	455(9)	456(10)	198(8)	184(8)	138(8)
C(45)	277(8)	369(8)	521(11)	27(8)	-22(7)	197(7)
C(46)	522(11)	700(12)	326(9)	104(8)	55(8)	459(10)
C(47)	391(9)	693(11)	541(11)	426(10)	260(9)	380(9)

III. Nuclear Magnetic Resonance Spectra

Figure 5. ^1H NMR spectrum of **1** in CDCl_3 .

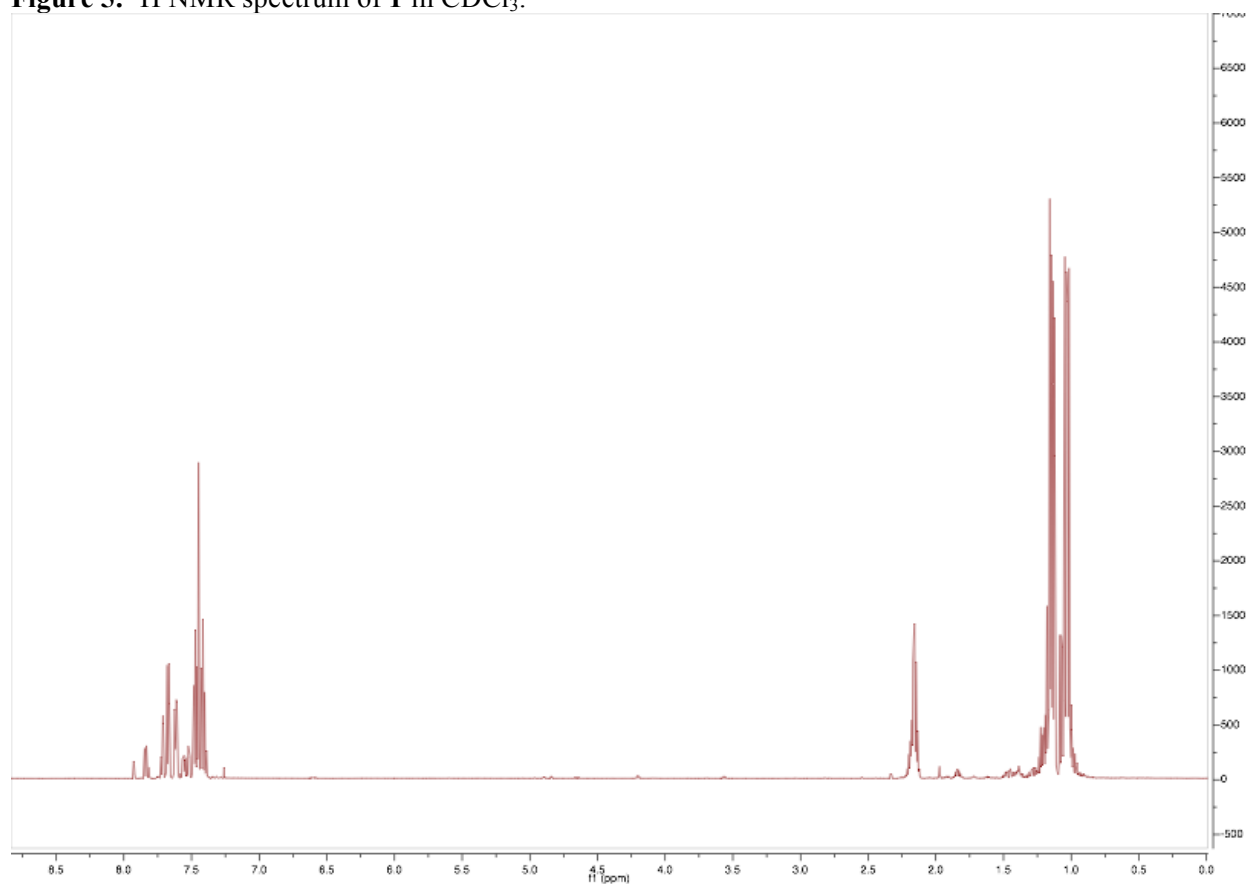


Figure 6. $^{31}\text{P}\{^1\text{H}\}$ NMR spectrum of **1** in C_6D_6 .

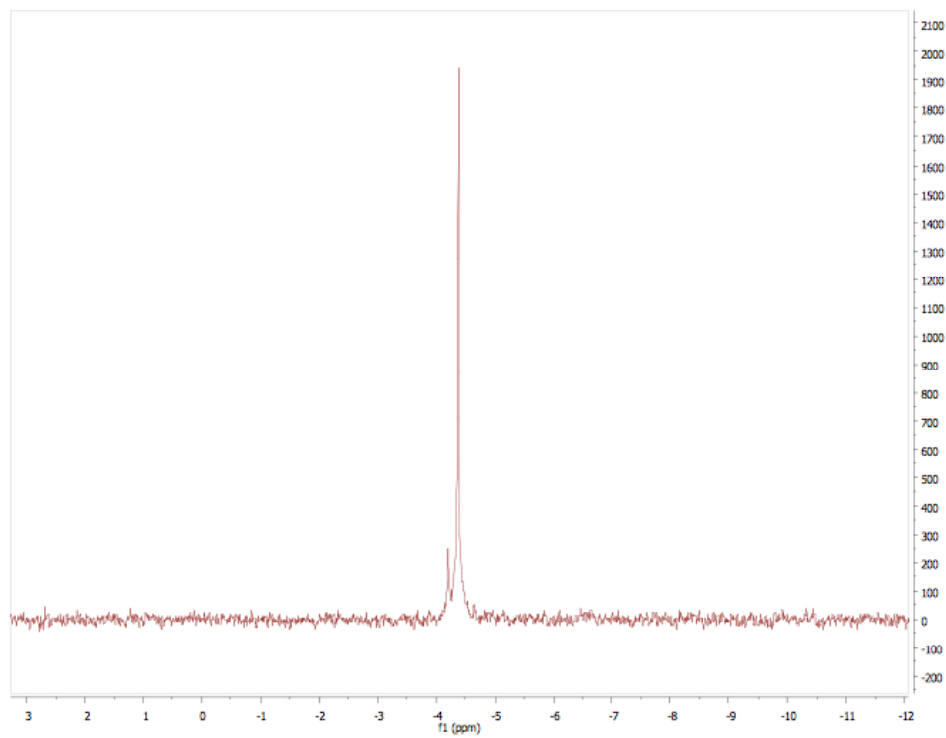


Figure 7. $^{13}\text{C}\{^1\text{H}\}$ NMR spectrum of **1** in CDCl_3 .

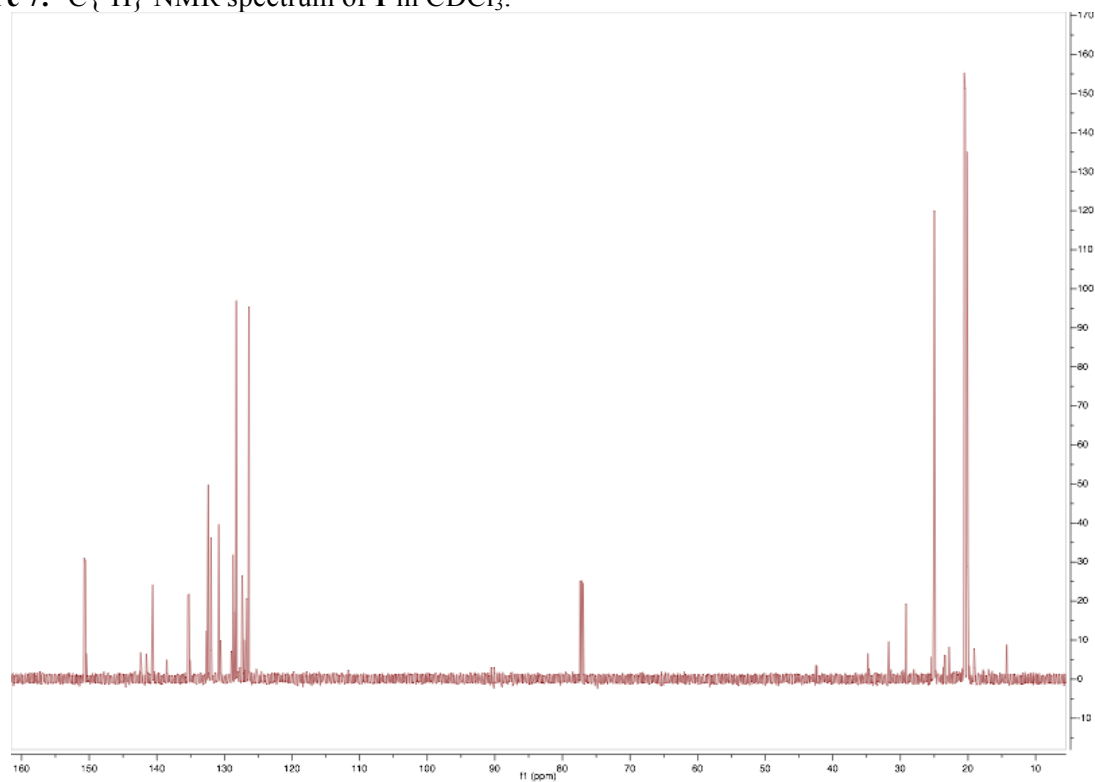


Figure 8. gHSQC of **1** in CDCl_3

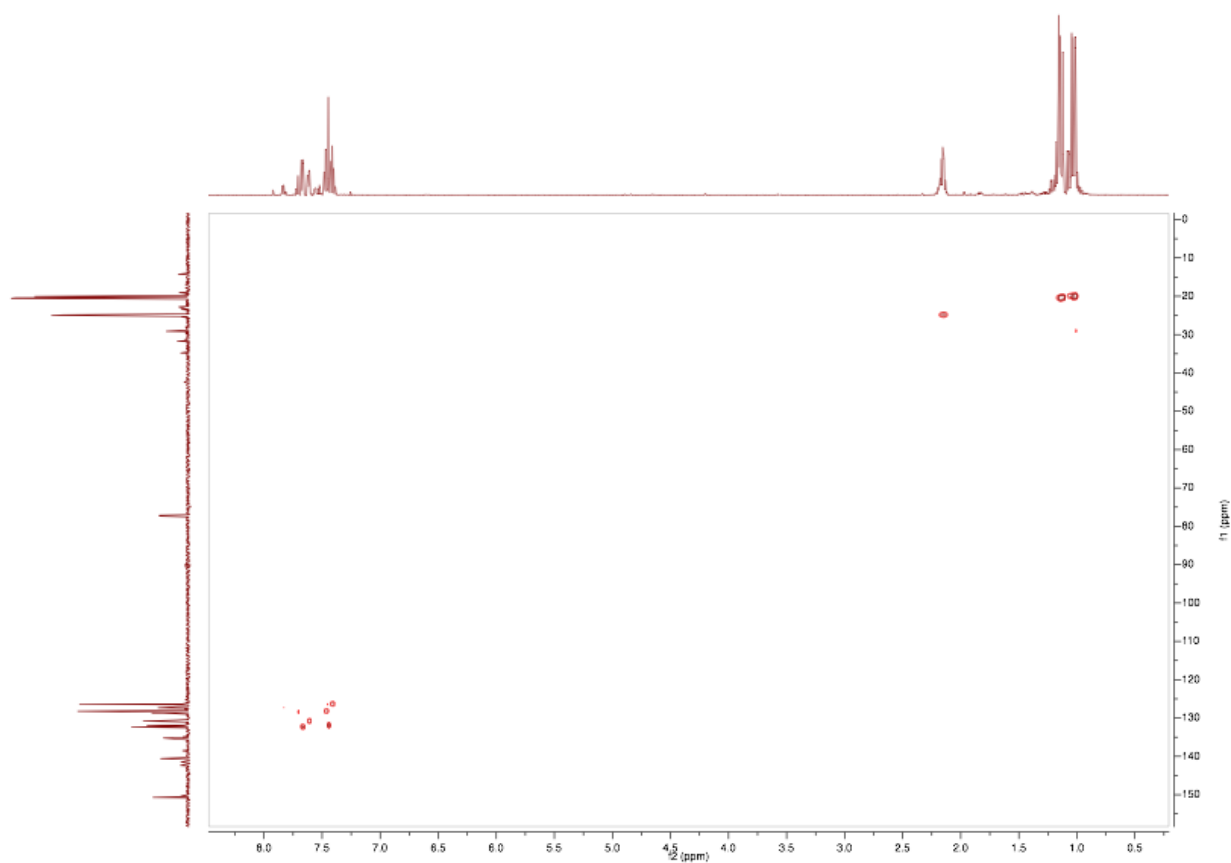


Figure 9. gHMBC of **1** in CDCl₃

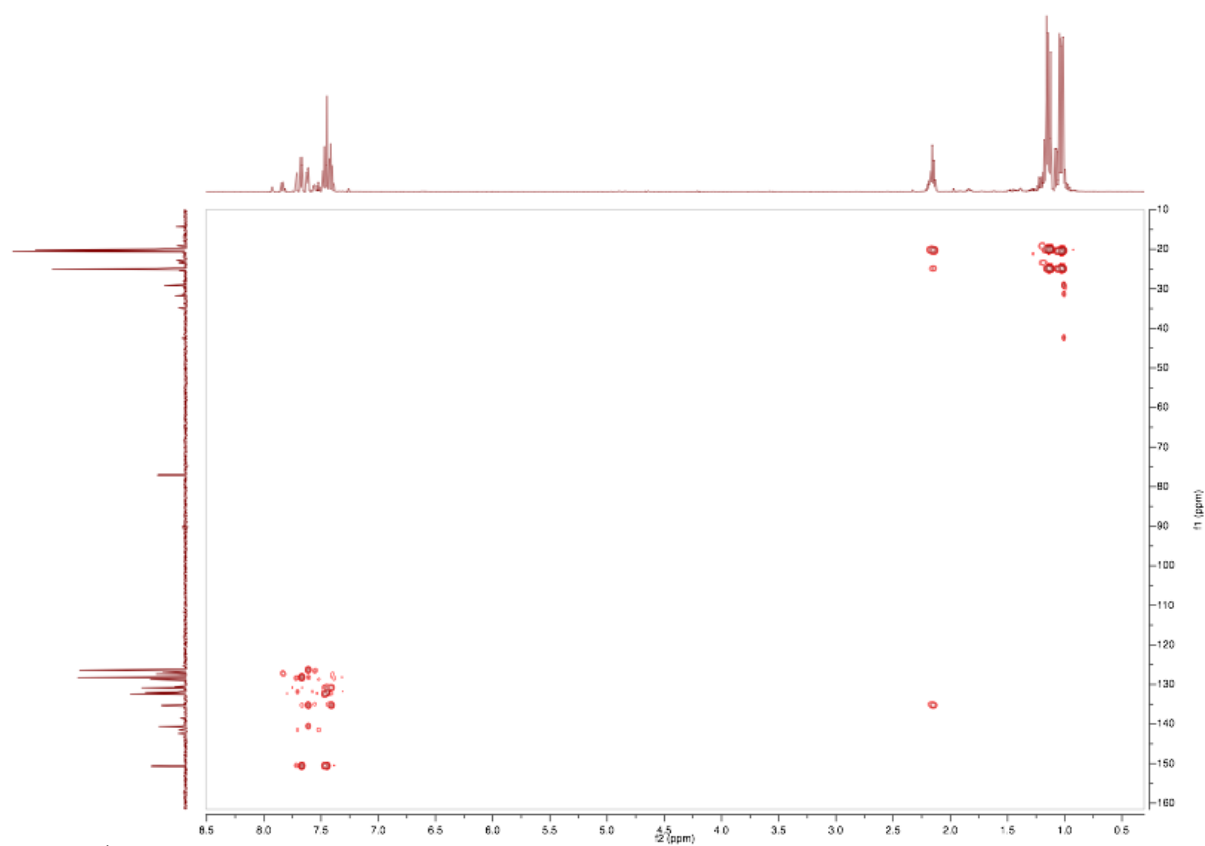


Figure 10. ¹H NMR spectrum of **2** in C₆D₆.

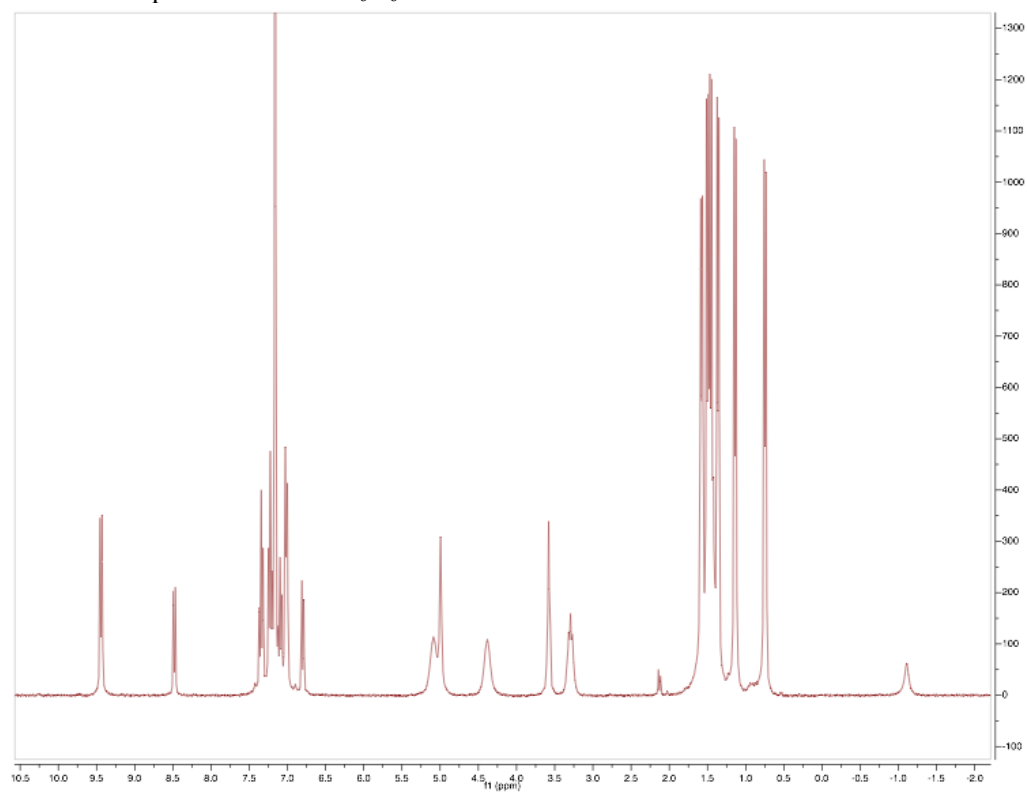


Figure 11. $^{13}\text{C}\{^1\text{H}\}$ NMR spectrum of **2** in C_6D_6 .

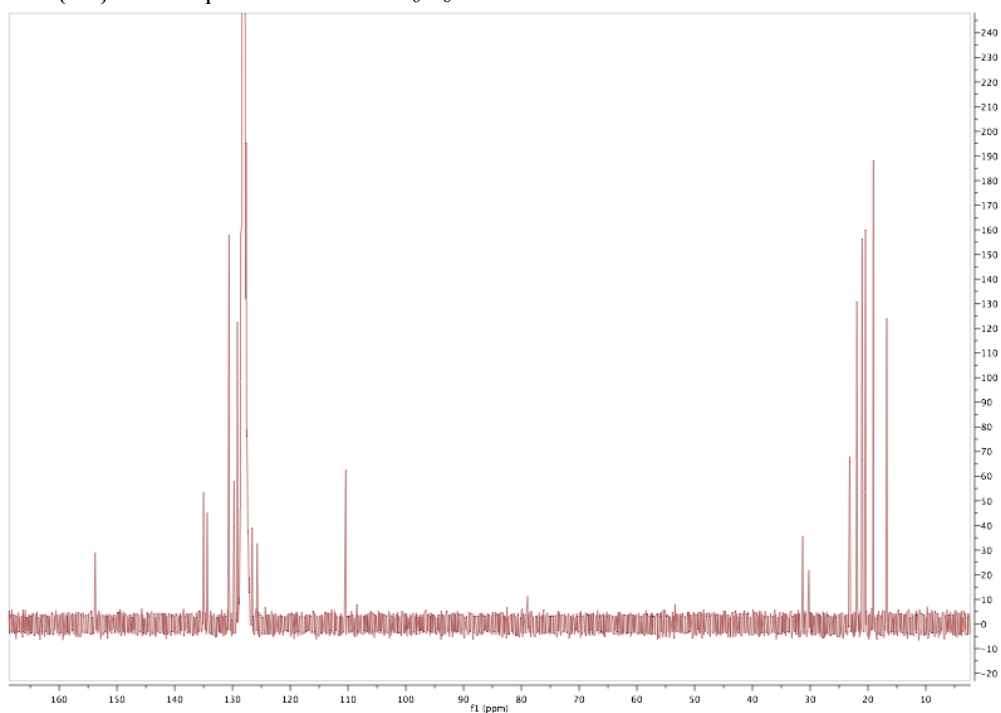
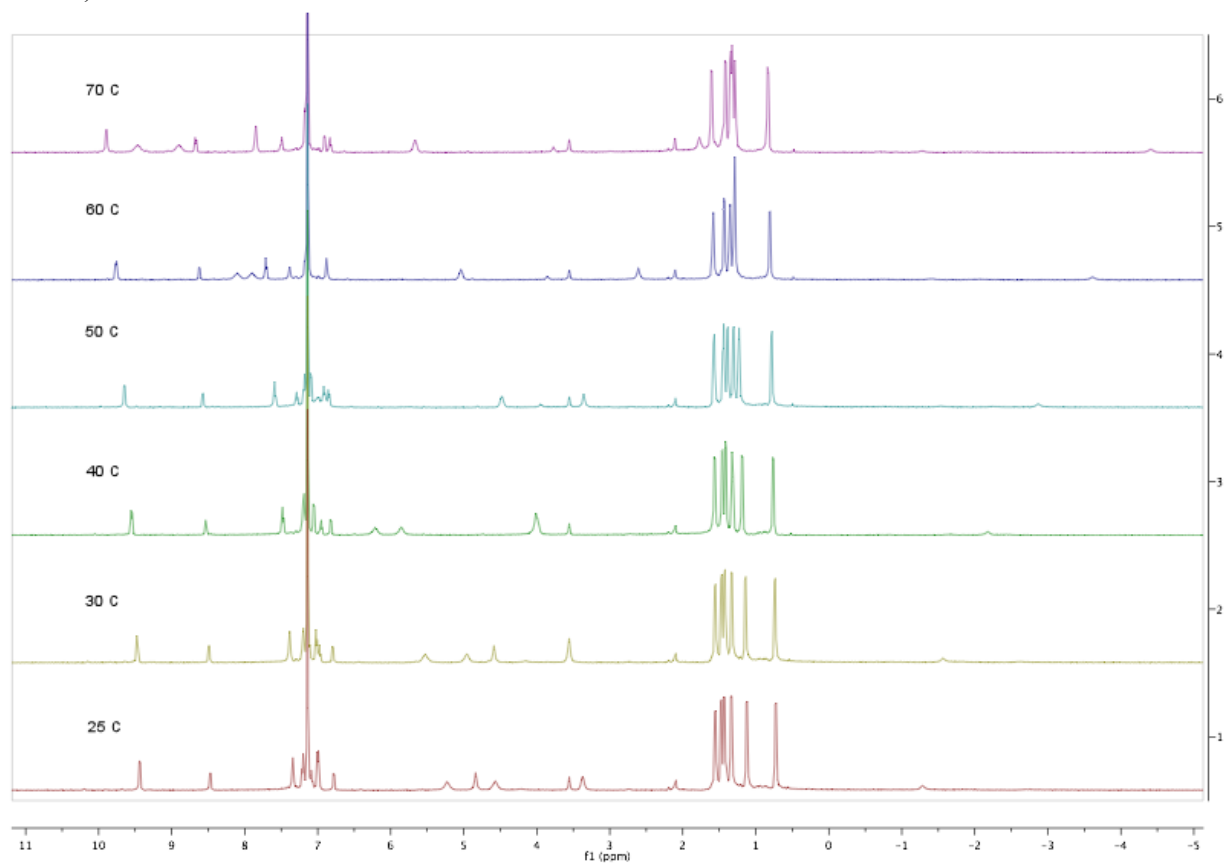


Figure 12. Variable temperature ^1H NMR spectra of **2** in C_6D_6 (25-70°C, top) and CD_2Cl_2 (-85°C-25°C, bottom)



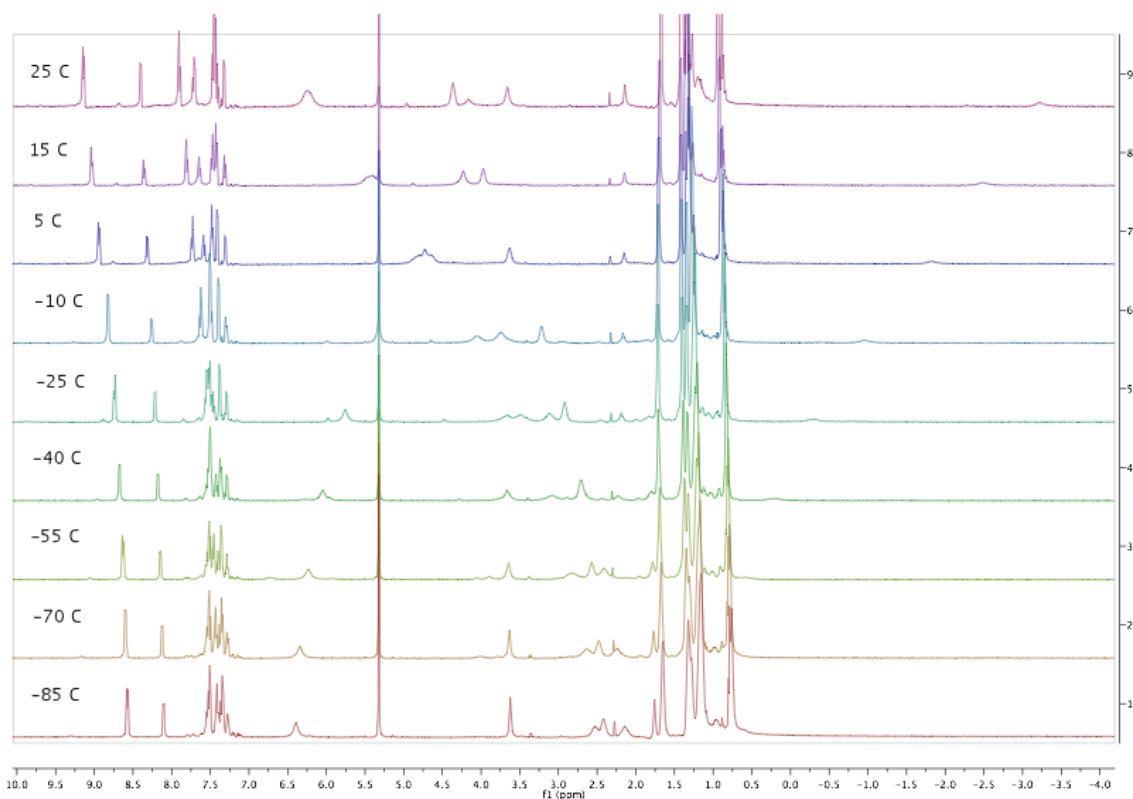


Figure 13. ^1H NMR spectra of **2-d₃** in C_6D_6

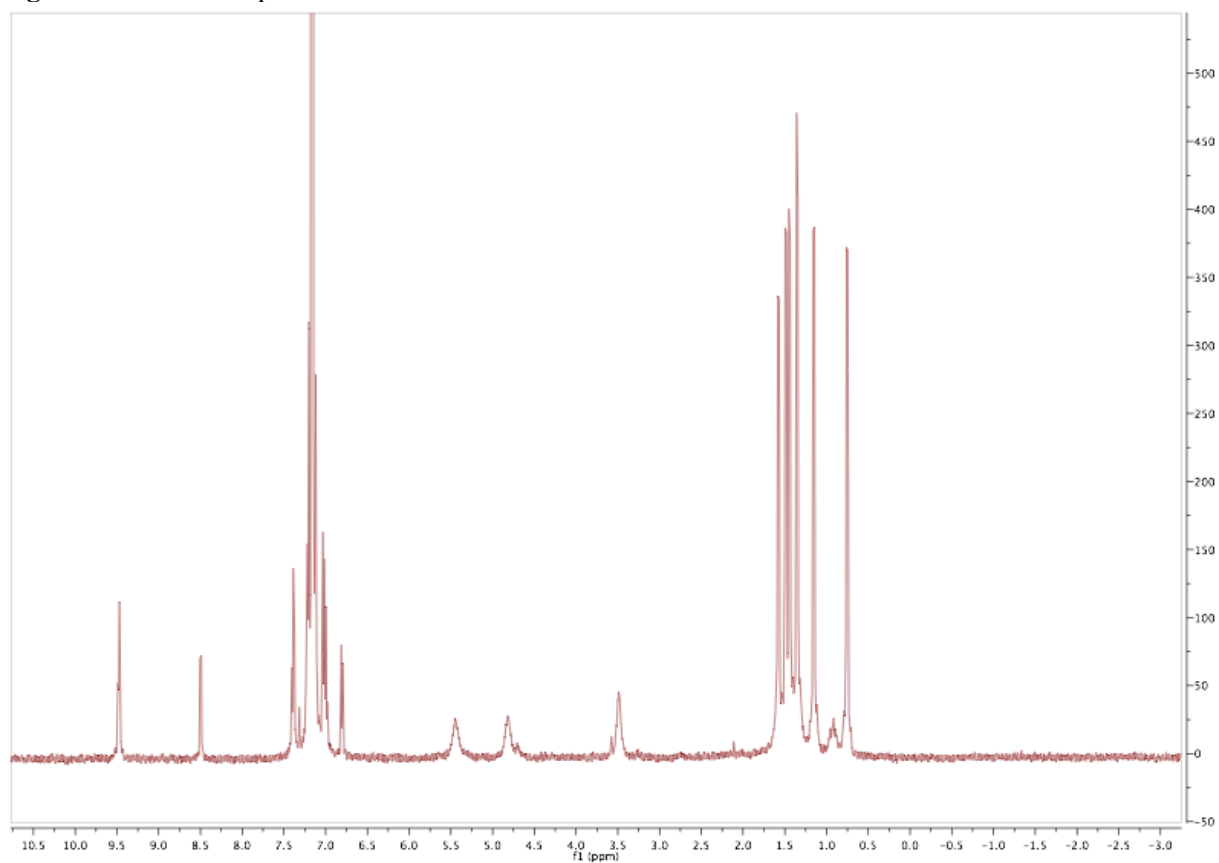


Figure 14. $^{31}\text{P}\{^1\text{H}\}$ NMR spectrum of **2** in CD_2Cl_2 at -70°C and -85°C .

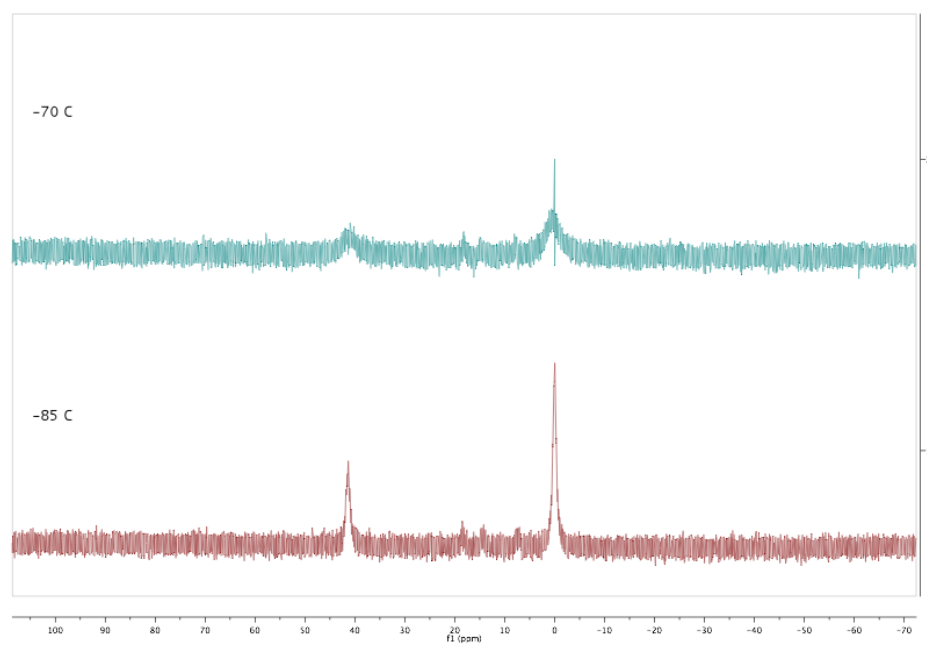


Figure 15. gCOSY of **2** in C_6D_6 .

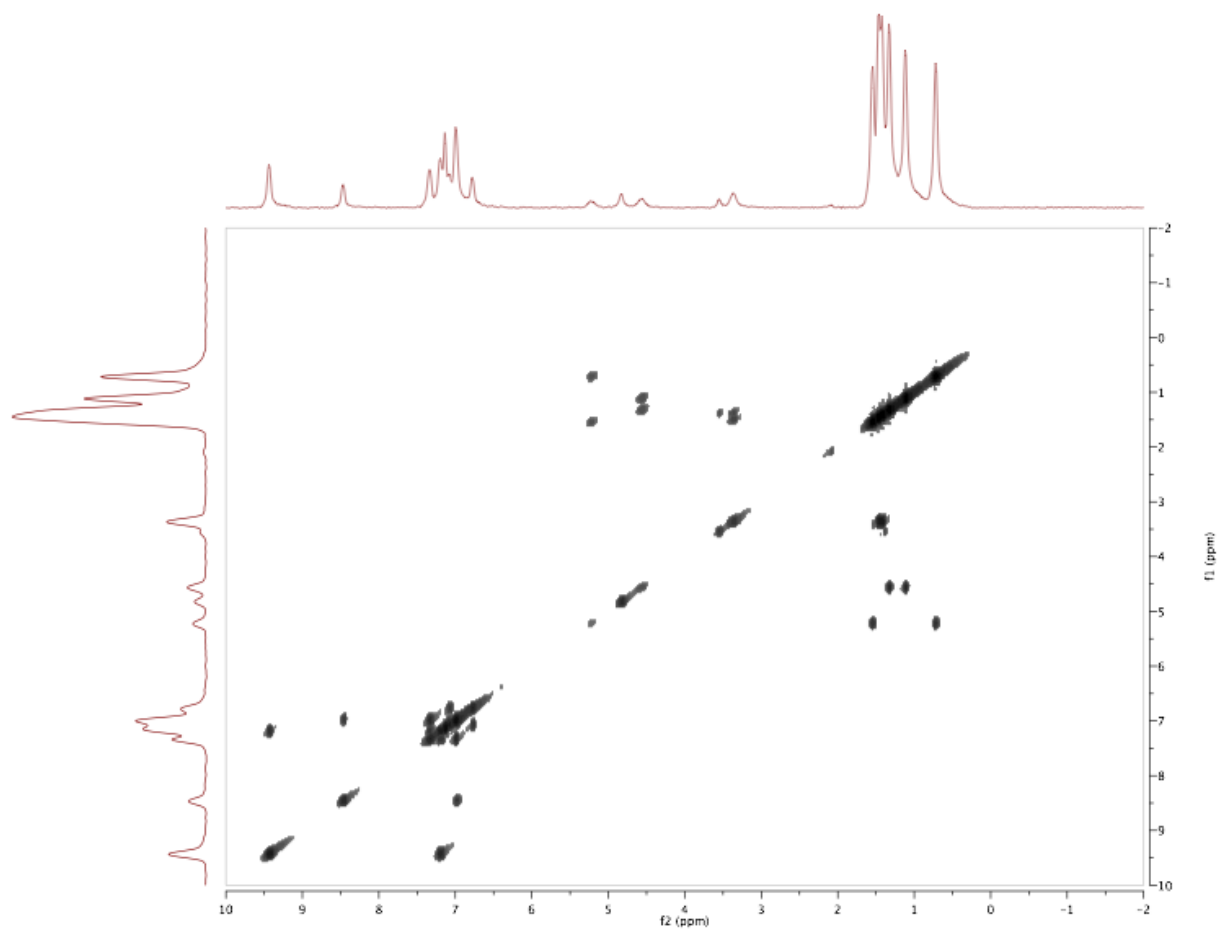


Figure 16. ^1H NMR spectrum of **3** in CD_2Cl_2 .

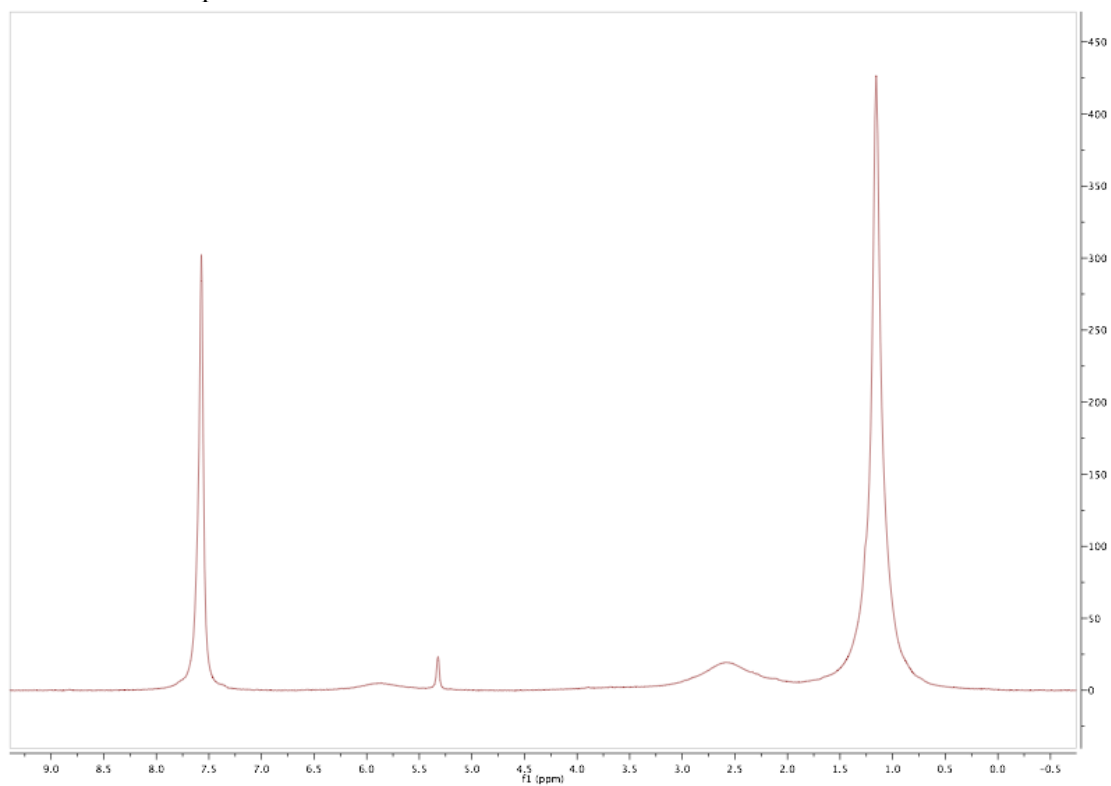


Figure 17. $^{31}\text{P}\{^1\text{H}\}$ NMR spectrum of **3** in CD_2Cl_2 .

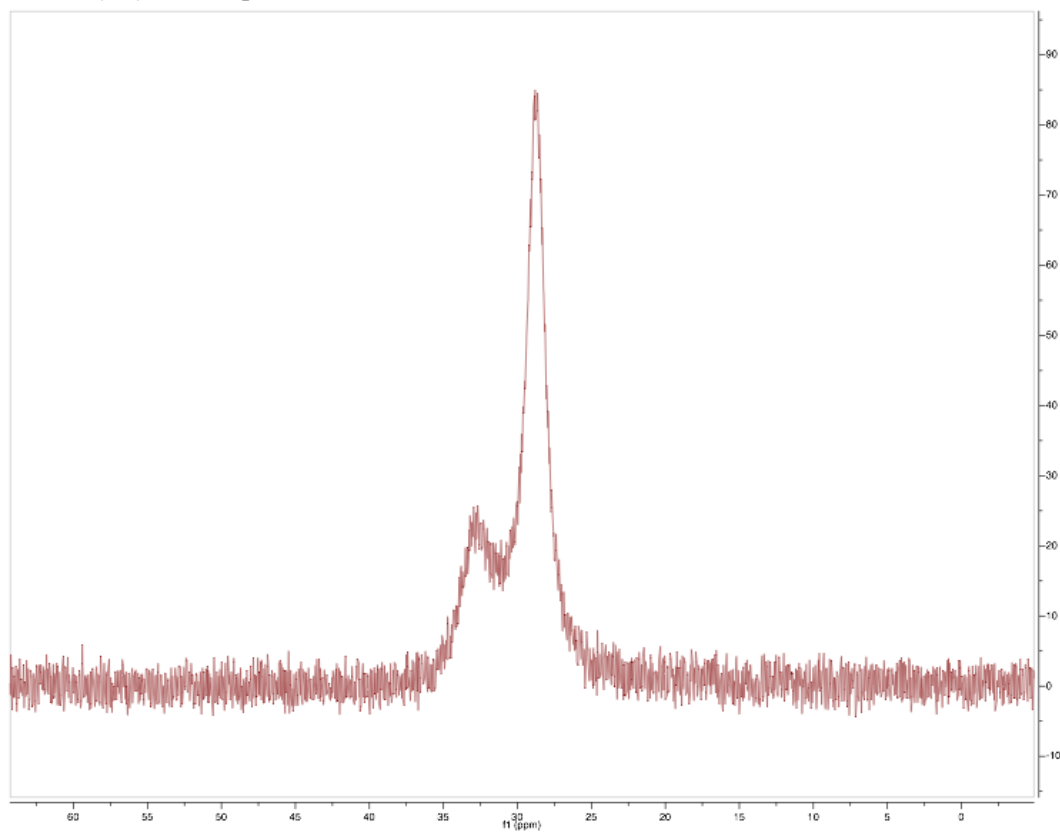


Figure 18. $^{13}\text{C}\{^1\text{H}\}$ NMR spectrum of **3** in CD_2Cl_2 at 40°C .

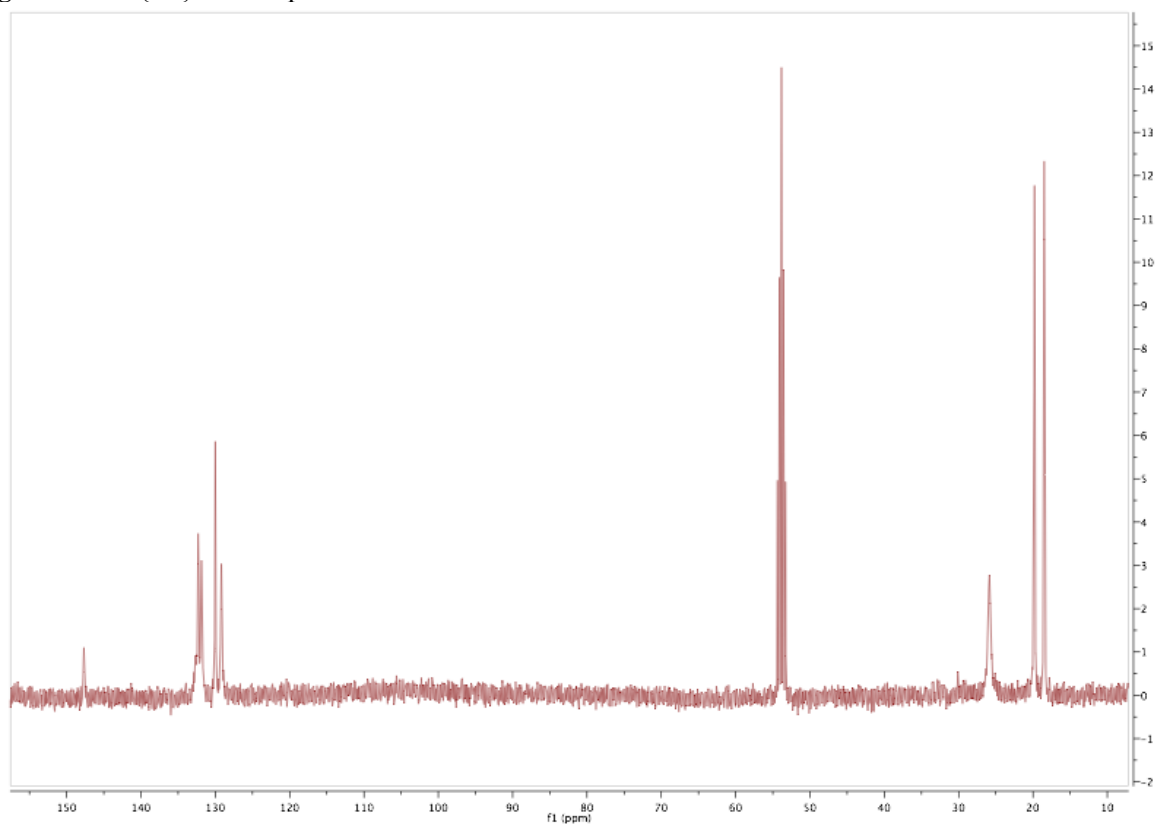
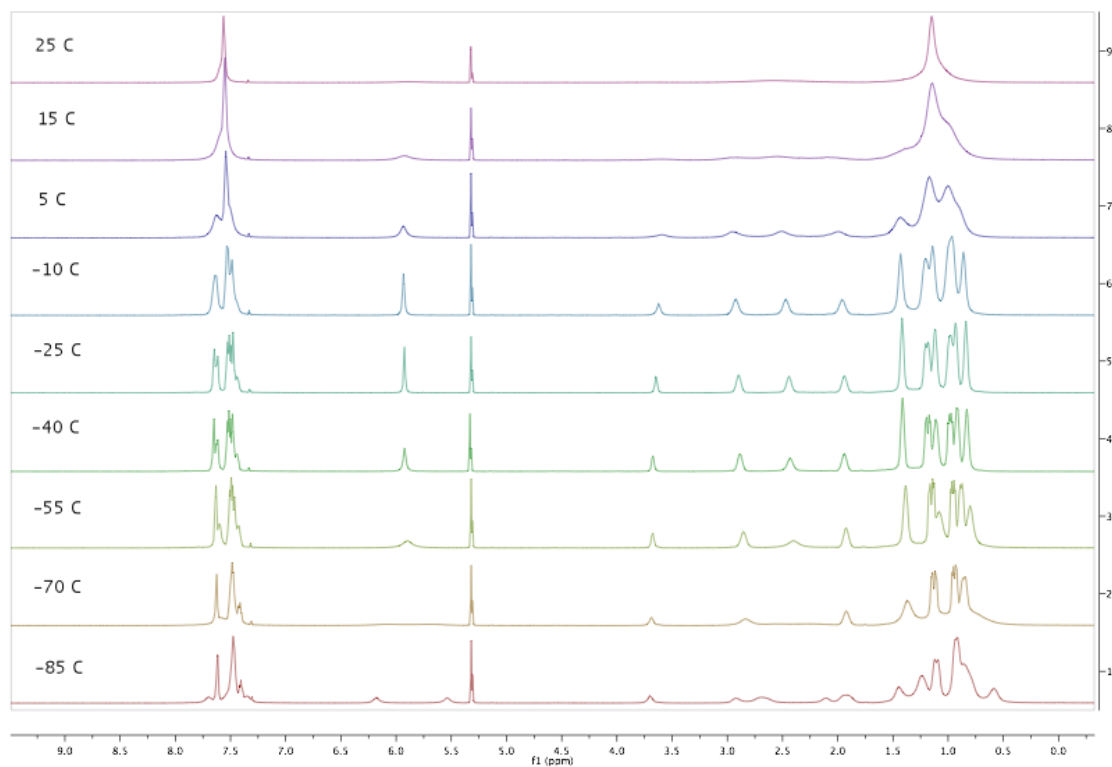


Figure 19. Variable temperature ^1H NMR spectra of **3** in CD_2Cl_2 (-85 – 25°C , top) and $\text{C}_6\text{D}_5\text{Br}$ (40 – 115°C , bottom).



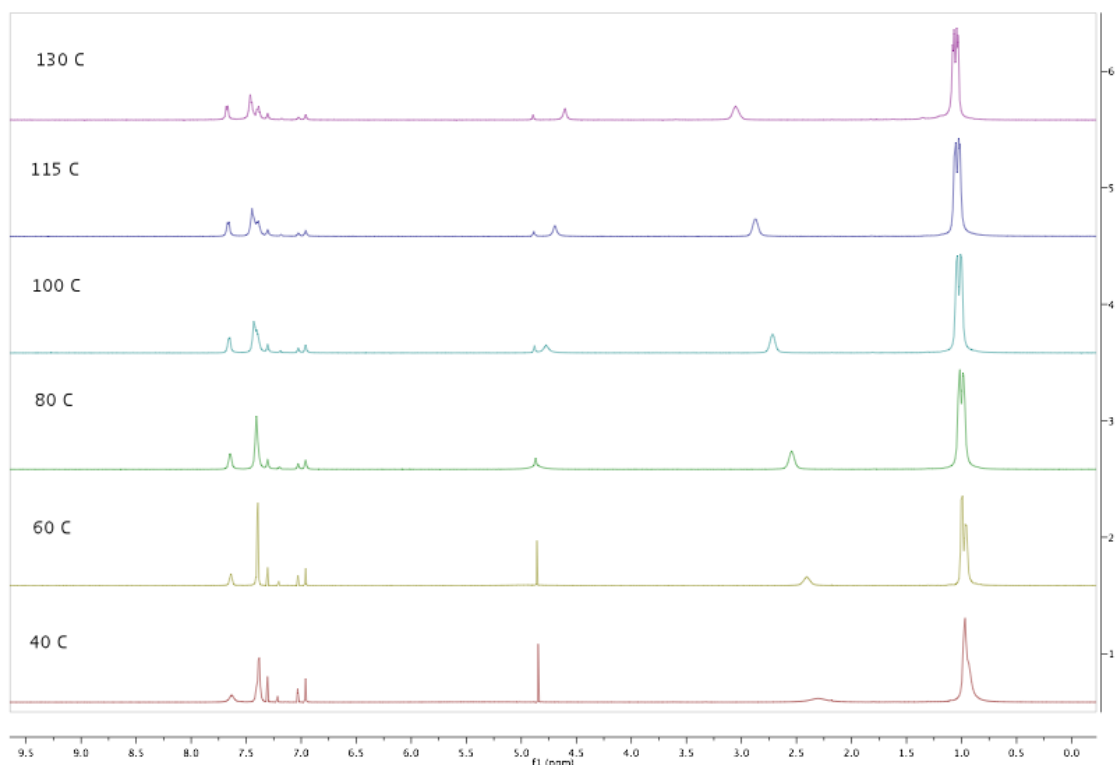
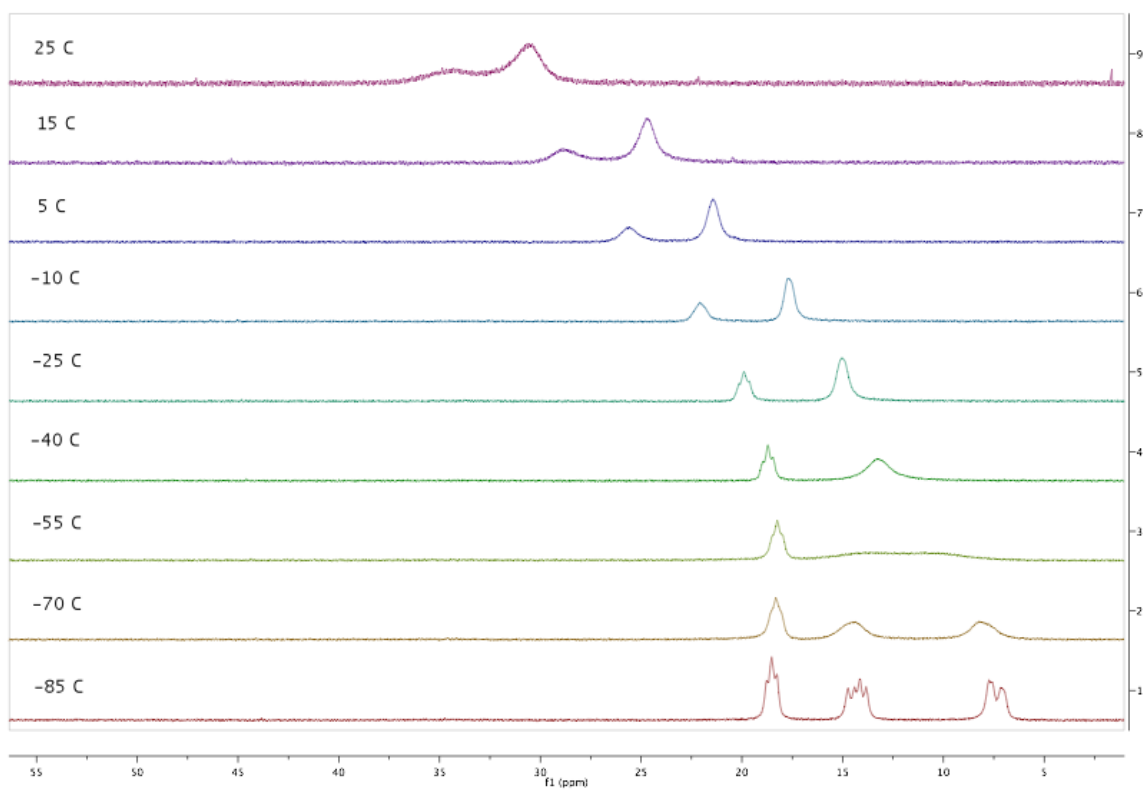


Figure 20. Variable temperature $^{31}\text{P}\{^1\text{H}\}$ NMR spectra of **3** in CD_2Cl_2 (-85-25°C, top) and $\text{C}_6\text{D}_5\text{Br}$ (40-130°C, bottom).



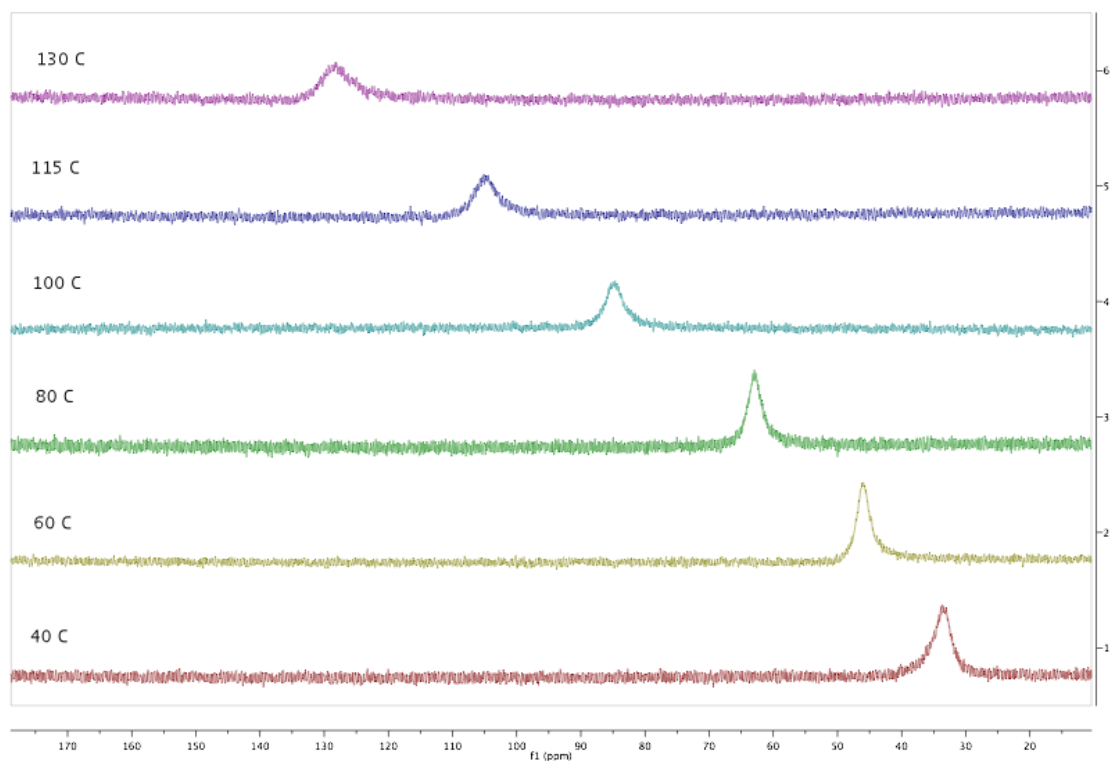


Figure 21. Variable temperature ^1H NMR spectra of **3-d₃** in CD_2Cl_2 (-85°C-25°C)

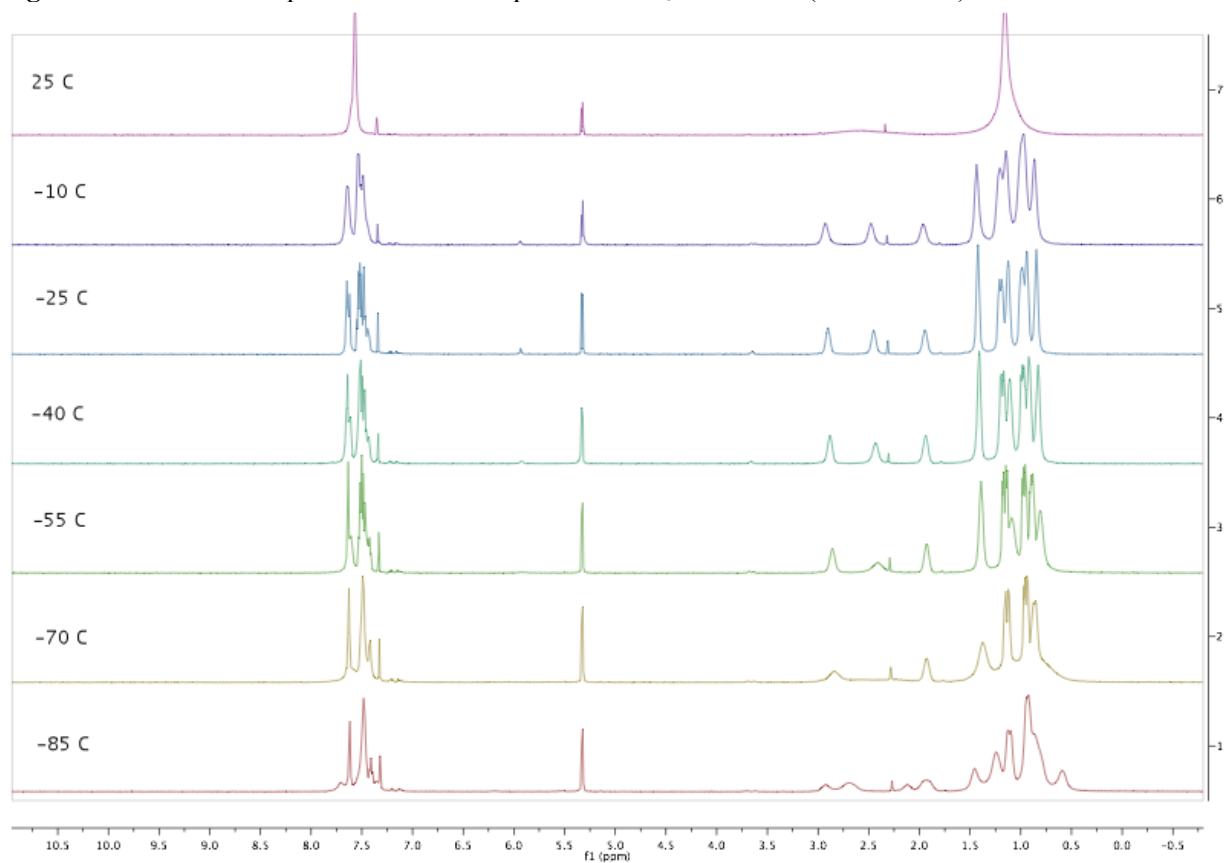


Figure 22. ^1H NMR spectrum of 1,3-bis(2'-bromophenyl)benzene in C_6D_6

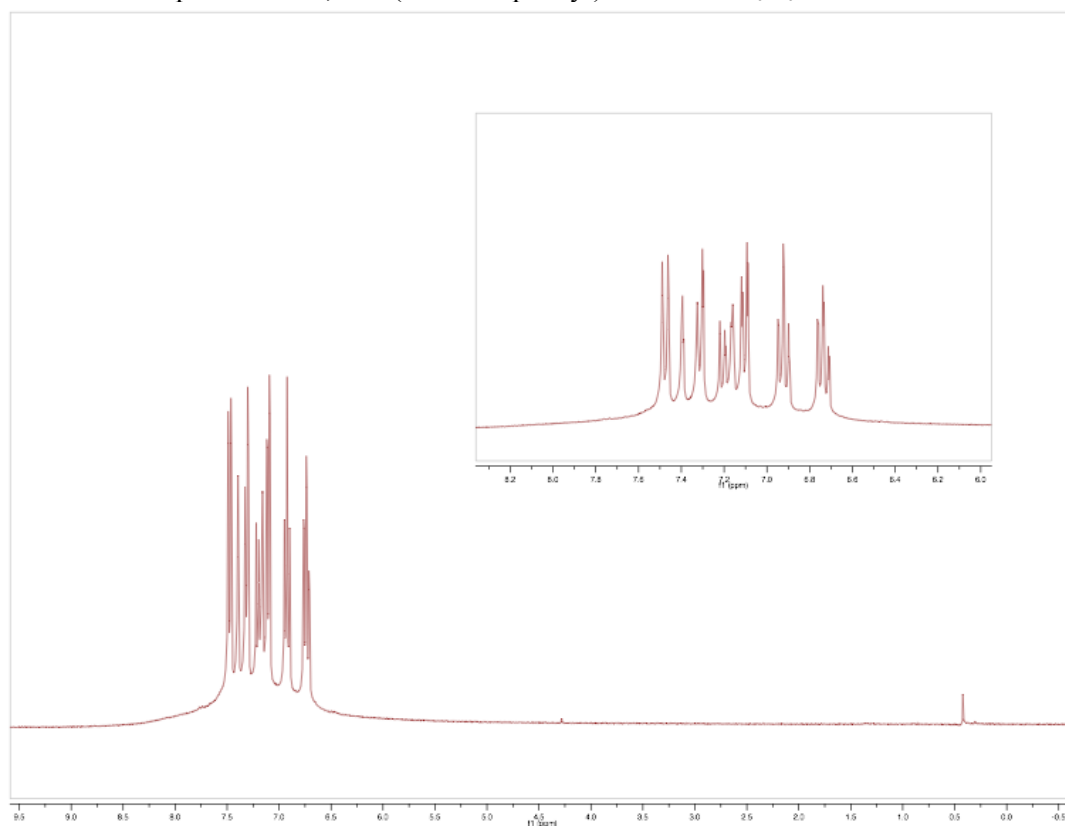


Figure 23. $^{13}\text{C}\{^1\text{H}\}$ NMR spectrum of 1,3-bis(2'-bromophenyl)benzene in CDCl_3

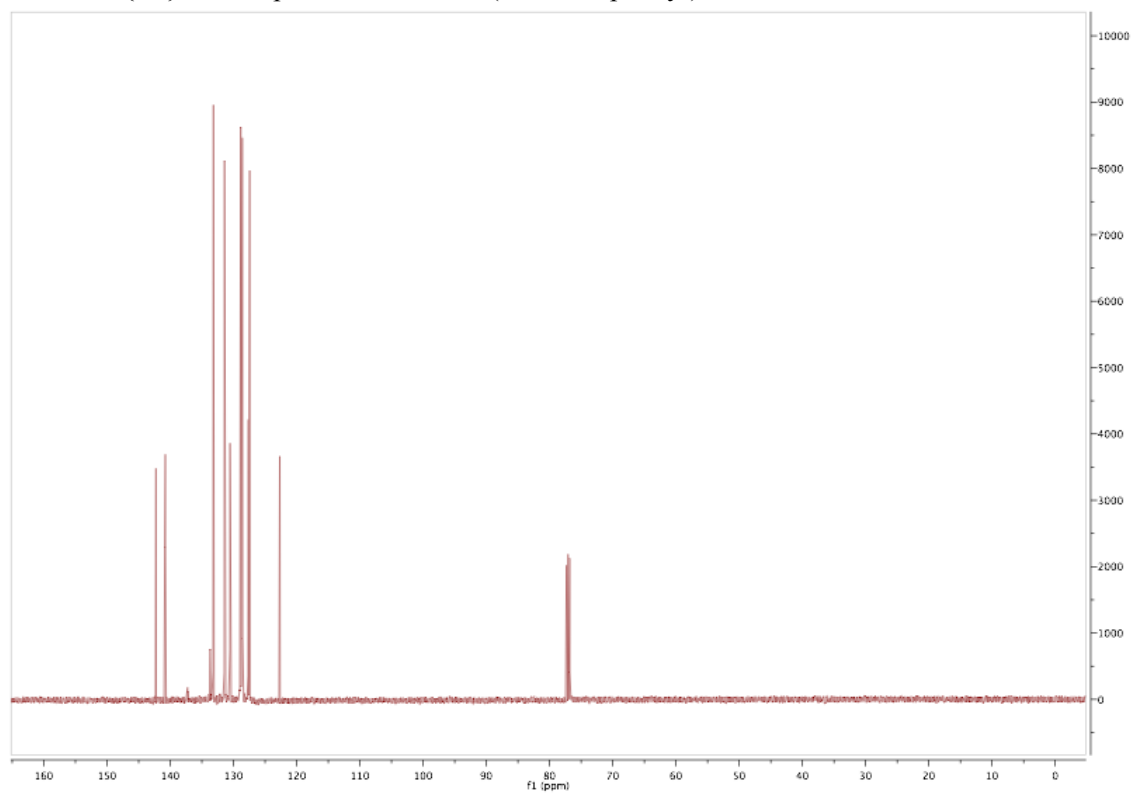


Figure 24. ^1H NMR spectrum of **4** in CD_2Cl_2

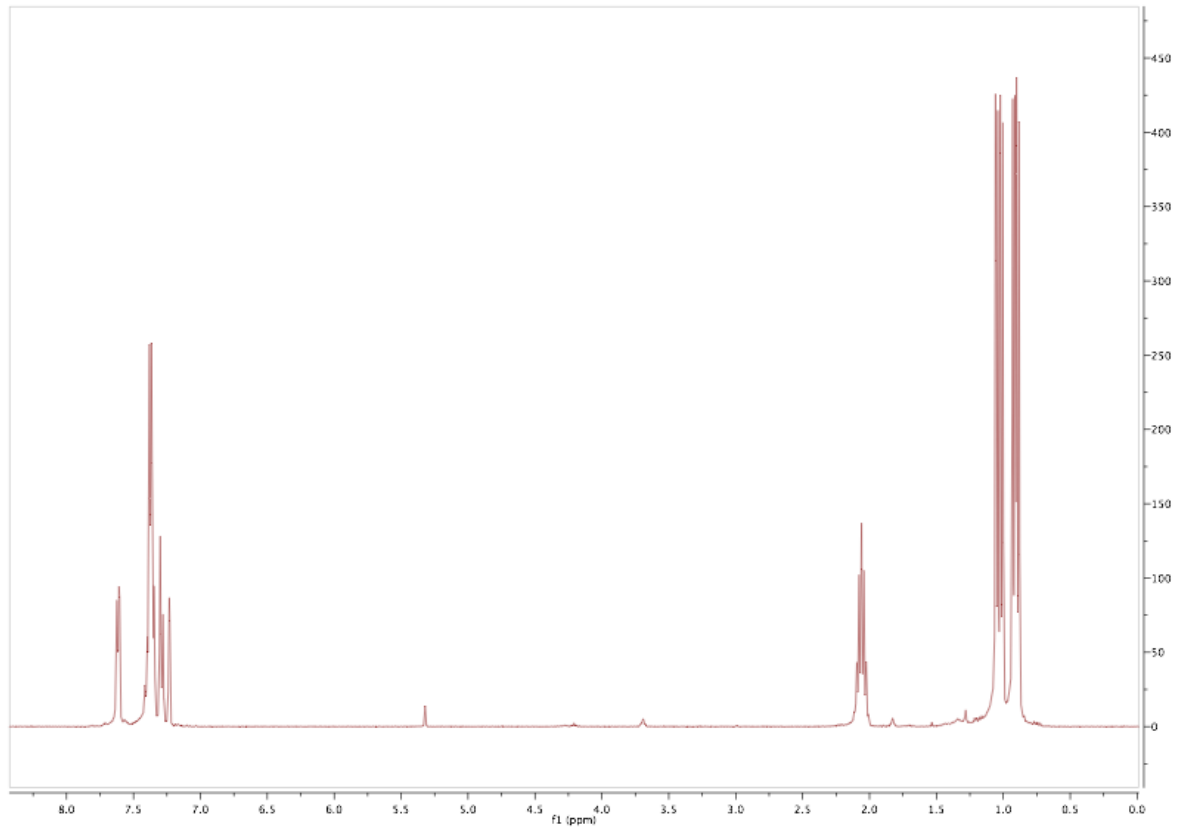


Figure 25. $^{31}\text{P}\{^1\text{H}\}$ NMR spectrum of **4** in C_6D_6

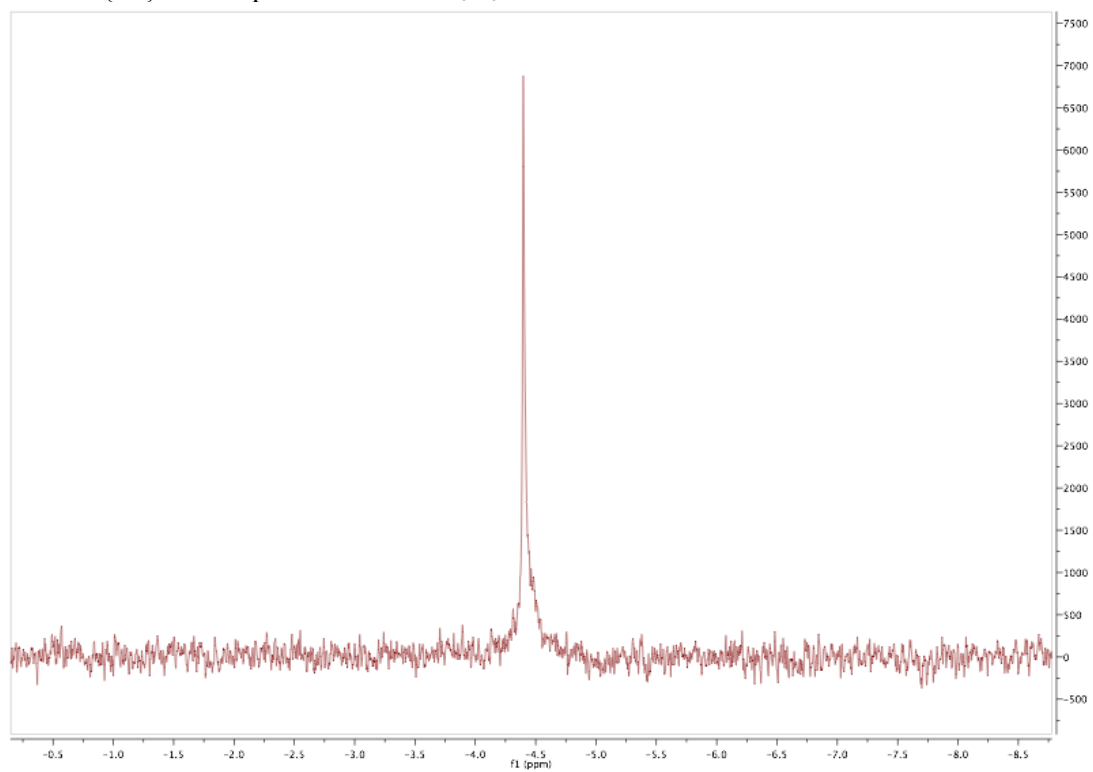


Figure 26. $^{13}\text{C}\{^1\text{H}\}$ NMR spectrum of **4** in CD_2Cl_2

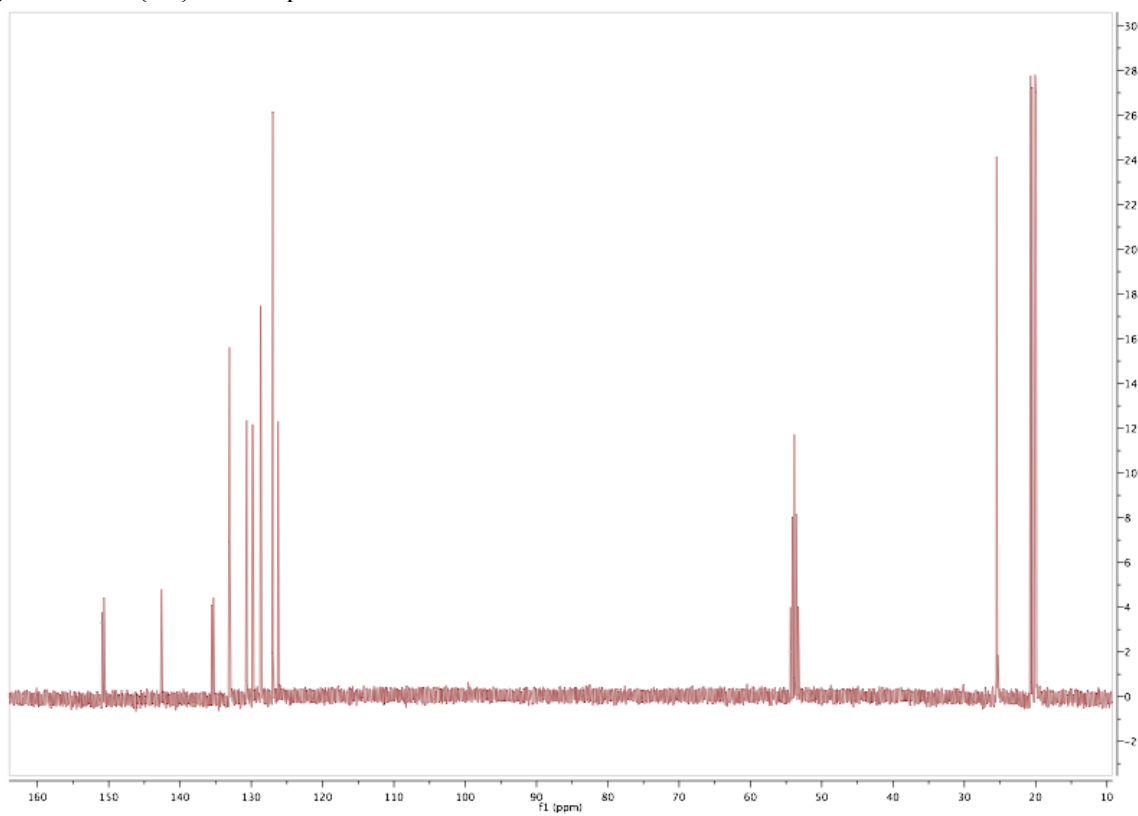
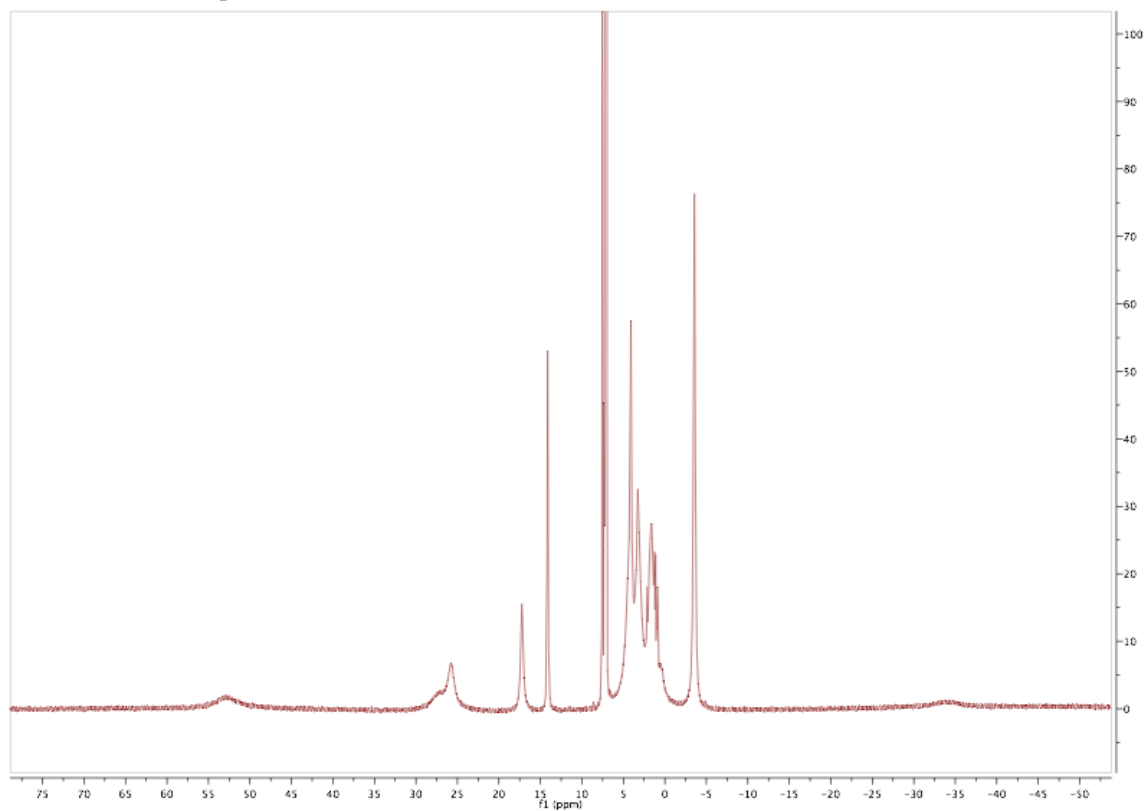


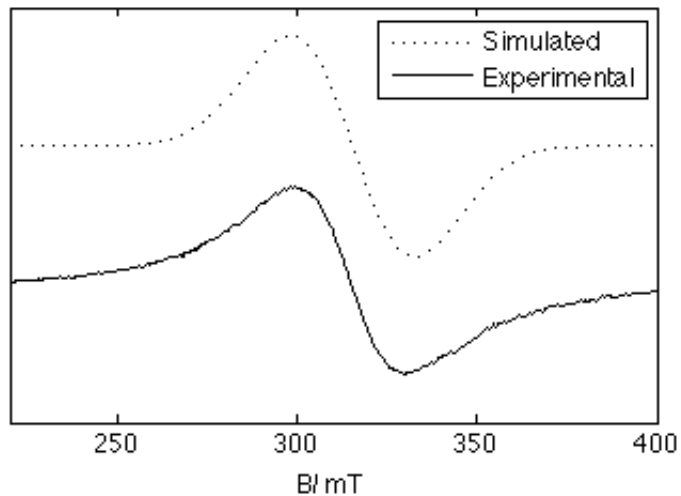
Figure 27. ^1H NMR spectrum of **5** in C_6D_6



IV. Electron Paramagnetic Resonance

Method: EPR samples were made as 5 mM solutions in 1:1 MeCN/toluene. Spectra were obtained at room temperature on a Bruker EMX Biospin spectrometer. EPR parameters were simulated with EasySpin.⁵ The EPR spectrum of **5** displays a g_{iso} value of 2.23, and ^{31}P hyperfine coupling was not measurable.

Figure 28. EPR spectrum and simulation of **5**



V. Computational Details

Method: All calculations were performed with density functional theory as implemented in Jaguar 7.0 (Schrodinger). Crystal structures of **2** and **5** were modified by truncating the isopropyl substituents to methyl groups, yielding initial structures for **2-Me** and **5-Me**, respectively. These structures were geometry optimized using the B3LYP functional^{6,7} and a custom basis set. Nickel was represented with a modified Los Alamos LACVP basis set^{8,9} (often referred to as LACV3P), in which the exponents are decontracted to match the effective core potential with triple- ξ quality basis. All other atoms were represented with the 6-311G**+ basis set. **2-Me** was optimized as a C_s -symmetric, unrestricted singlet, and **5-Me** was optimized without symmetry constraints as an unrestricted doublet. All geometric minima were confirmed to lack imaginary frequency vibrations. Molecular orbitals were visualized with Molden using an isosurface value of 0.05.

Table 11. Optimized coordinates of 2-Me.

Ni	-0.2080558326	-2.6076043060	0.0000000000
Ni	-0.1802653003	2.5764085068	0.0000000000
Cl	0.9120770074	-4.6097066475	0.0000000000
Cl	-2.1949171329	3.4793812472	0.0000000000
P	1.3007123043	4.1587774998	0.0000000000
C	1.2816589501	1.2930059083	0.0000000000
C	-0.8890097392	-0.6858756891	0.0000000000
H	-1.9685161624	-0.8501357153	0.0000000000
C	2.8827457938	3.2185083257	0.0000000000
C	4.1767641354	3.7485301336	0.0000000000
H	4.3318257956	4.8223635363	0.0000000000
C	5.0852642857	1.5132411695	0.0000000000
C	3.7986417226	0.9813240830	0.0000000000
H	3.6530290418	-0.0932920509	0.0000000000
C	2.6854174959	1.8290411361	0.0000000000
C	5.2769222976	2.8960132598	0.0000000000
H	6.2808358201	3.3051613468	0.0000000000
H	5.9425528227	0.8494125915	0.0000000000
P	-0.4545745639	-2.8580706877	2.2191868668
C	0.6708143545	0.8198635076	1.2285314573
H	1.0547146585	1.1985220254	2.1696241027
C	-0.4237036634	-0.0074195150	1.2297462852
C	-1.1850025267	-0.2109588387	2.4899906036
C	-1.7871136926	0.8883506617	3.1167863375
H	-1.7104582332	1.8640282990	2.6514818517
C	-2.5211363369	0.7198141858	4.2866537302
H	-2.9924595137	1.5785135307	4.7510805515
C	-2.6686328438	-0.5476282105	4.8461499858
H	-3.2453258738	-0.6814365942	5.7543307752
C	-2.0740624300	-1.6469206456	4.2328267558
H	-2.1884223448	-2.6271326995	4.6807537200
C	-1.3317005888	-1.4898523842	3.0579480088
C	-1.3899875558	-4.3816978081	2.6491062227
H	-1.4149756890	-4.5542312835	3.7272549038
C	1.1197496861	-3.0277836554	3.1608516184
H	1.6823981430	-3.8596222036	2.7360397462

C	1.3949675501	5.3089493816	1.4382129244
P	-0.4545745639	-2.8580706877	-2.2191868668
C	0.6708143545	0.8198635076	-1.2285314573
H	1.0547146585	1.1985220254	-2.1696241027
C	-0.4237036634	-0.0074195150	-1.2297462852
C	-1.1850025267	-0.2109588387	-2.4899906036
C	-1.7871136926	0.8883506617	-3.1167863375
H	-1.7104582332	1.8640282990	-2.6514818517
C	-2.5211363369	0.7198141858	-4.2866537302
H	-2.9924595137	1.5785135307	-4.7510805515
C	-2.6686328438	-0.5476282105	-4.8461499858
H	-3.2453258738	-0.6814365942	-5.7543307752
C	-2.0740624300	-1.6469206456	-4.2328267558
H	-2.1884223448	-2.6271326995	-4.6807537200
C	-1.3317005888	-1.4898523842	-3.0579480088
C	-1.3899875558	-4.3816978081	-2.6491062227
H	-1.4149756890	-4.5542312835	-3.7272549038
C	1.1197496861	-3.0277836554	-3.1608516184
H	1.6823981430	-3.8596222036	-2.7360397462
C	1.3949675501	5.3089493816	-1.4382129244
H	-2.4105122854	-4.3021178585	2.2714856511
H	-0.8957501633	-5.2194758601	2.1575984848
H	1.7023947537	-2.1124049307	3.0480893927
H	0.9241943620	-3.2010723063	4.2215272828
H	2.2462549722	5.9901305362	1.3592415933
H	0.4696973684	5.8869182808	1.4791009732
H	1.4801355685	4.7298744016	2.3583942656
H	-0.8957501633	-5.2194758601	-2.1575984848
H	-2.4105122854	-4.3021178585	-2.2714856511
H	0.9241943620	-3.2010723063	-4.2215272828
H	1.7023947537	-2.1124049307	-3.0480893927
H	2.2462549722	5.9901305362	-1.3592415933
H	1.4801355685	4.7298744016	-2.3583942656
H	0.4696973684	5.8869182808	-1.4791009732

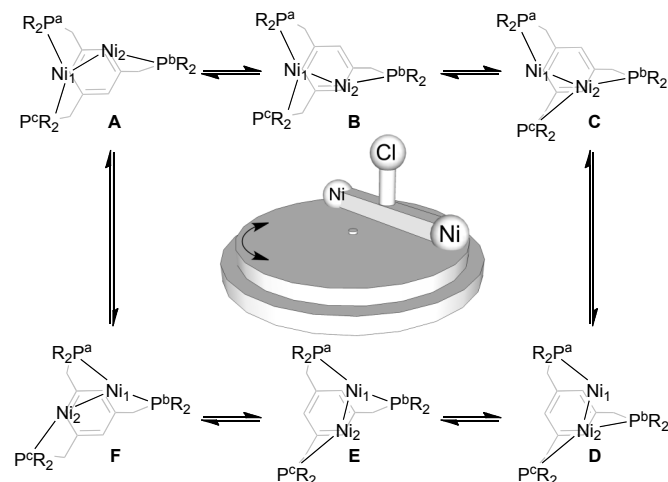
Table 12. Optimized coordinates of 5-Me.

Ni	6.3908431035	-0.1145296960	11.5200180168
Cl	8.3322717860	-1.1988605041	10.7650175997
P	5.3035752537	-2.0377525661	12.0396571209
P	7.0113353331	1.9257817090	10.7433714660
C	3.6128087285	-1.9936661009	12.8001581602
C	2.7022999439	-3.0397302992	12.5977090895
H	2.9719466255	-3.8730335239	11.9605388335
C	1.4485770255	-3.0400063129	13.2013192894
H	0.7630118103	-3.8607267645	13.0232751099
C	1.0857979081	-1.9871309639	14.0357060607
H	0.1133208066	-1.9759792433	14.5145536668
C	1.9773016648	-0.9410402543	14.2494781332
H	1.6952549709	-0.1141025741	14.8915372992
C	3.2367776138	-0.9204107073	13.6360520368

C	4.1252340041	0.2524829945	13.9111820503
C	4.7425588344	0.3958912384	15.1576792725
H	4.6167965858	-0.3760449770	15.9083075866
C	5.5152564563	1.5207526558	15.4348229963
H	5.9947412731	1.6203265706	16.4020163299
C	5.6713605909	2.5208677432	14.4784974997
H	6.2671667909	3.3985615657	14.7016669437
C	5.0640190313	2.4007003219	13.2245551598
C	4.2996785074	1.2583767760	12.9512350846
H	3.7936576938	1.1740802607	11.9961245760
C	5.1704451599	3.5077562758	12.2228245777
C	4.4441321459	4.6802250298	12.4708395249
H	3.8367731132	4.7385702495	13.3671025207
C	4.4765401624	5.7523812425	11.5855397581
H	3.8987754026	6.6452916703	11.7954074573
C	5.2483338131	5.6674274611	10.4306877257
H	5.2811167285	6.4940966074	9.7301062970
C	5.9863583175	4.5150749428	10.1794542416
H	6.5907535969	4.4711955936	9.2816939702
C	5.9648540899	3.4241865274	11.0592268440
C	6.2526545458	-3.0944403831	13.2212824976
C	5.1365850663	-3.1385038157	10.5710109779
C	7.2603252190	1.8974562219	8.9170780602
C	8.6698448411	2.4546115841	11.3619769545
H	7.7871417257	2.7777988362	8.5421728345
H	7.8526744404	1.0058721257	8.7040051939
H	6.2972184139	1.8037279929	8.4126921564
H	9.0070633723	3.3738011434	10.8768814331
H	8.6223668458	2.6110653261	12.4406092321
H	9.3666081099	1.6387603348	11.1609234806
H	4.8449822504	-4.1585111028	10.8312423212
H	4.4134045828	-2.7169139117	9.8710042063
H	6.1163210530	-3.1552232098	10.0903834088
H	5.7781307172	-4.0685657945	13.3622592577
H	7.2579404371	-3.2151572006	12.8133754023
H	6.3285303178	-2.5860690415	14.1835331123

VI. Molecular Crank Illustration

Figure 29. Proposed mechanism of rotation of the Ni₂ core in **3** (bridging chloride omitted for clarity) and (center) schematic representation of the molecular crank.



References

- (1) Pangborn, A. B.; Giardello, M. A.; Grubbs, R. H.; Rosen, R. K.; Timmers, F. J. *Organometallics* **1996**, *15*, 1518-1520/.
- (2) Feng, X.; Wu, J.; Enkelmann, V.; Müllen, K. *Org. Lett.* **2006**, *8*, 1145-1148.
- (3) Tsui, E. Y.; Day, M. W.; Agapie, T. *Angew. Chem. Int. Ed.* **2011**, *50*, 1668-1672.
- (4) Feng, X.; Pisula, W.; Mullen, K. *J. Am. Chem. Soc.* **2007**, *129*, 14116-14117.
- (5) Stoll, S.; Schweiger, A., *J. Magn. Reson.*, **2006**, *178*, 42-55.
- (6) Becke, A. D., *J. Chem. Phys.*, **1993**, *98*, 5648-5652.
- (7) Stephens, P. J.; Devlin, F. J.; Chabalowski, C. F.; Frisch, M. J., *J. Phys. Chem.*, **1994**, *98*, 11623-11627.
- (8) Hay, P. J.; Wadt, W. R., *J. Chem. Phys.*, **1985**, *82*, 270-283.
- (9) Wadt, W. R.; Hay, P. J., *J. Chem. Phys.*, **1985**, *82*, 284-298.